Design, Synthesis, and validation of Imaging Probes

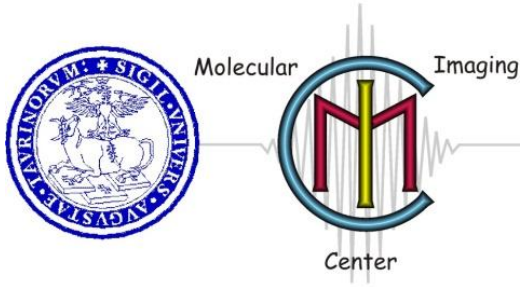

MRI CEST agents: basic principles, mechanism of action and classification

Enzo Terreno

Torino, September 19 to 30, 2011

Lesson outline

- CEST agents mechanism of action
- Sensitivity issue
- CEST agents vs conventional MRI agents
- CEST agents classification
- LIPOCEST

CEST (Chemical Exchange Saturation Transfer) agents

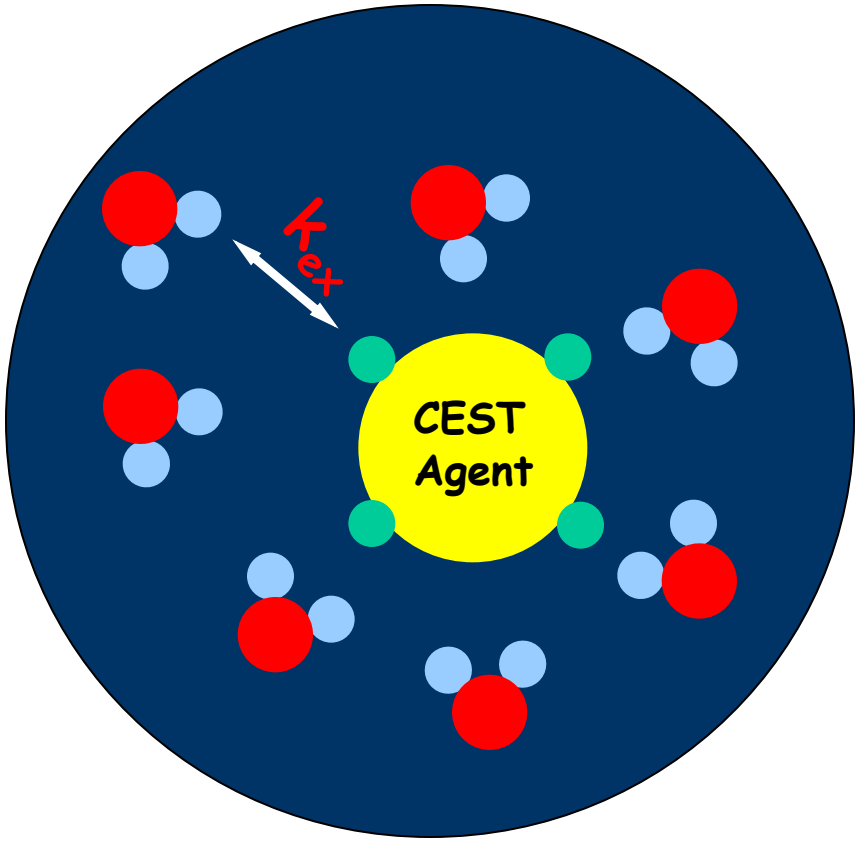

$\Delta\omega$ (rad·Hz) = ω_{WAT} - ω_{CEST}

If $\Delta\omega > k_{ex}$ then….

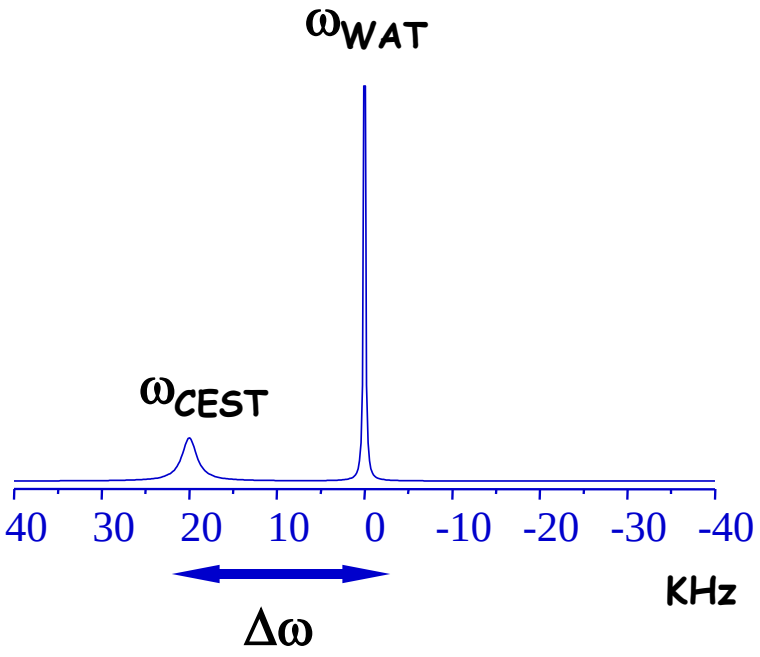

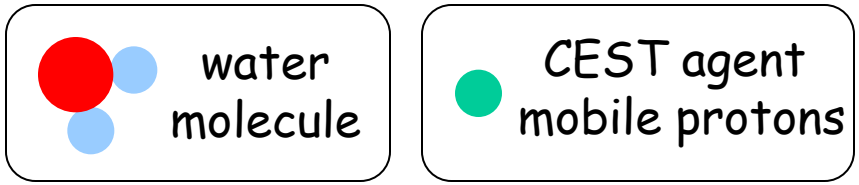

The MR-CEST experiment

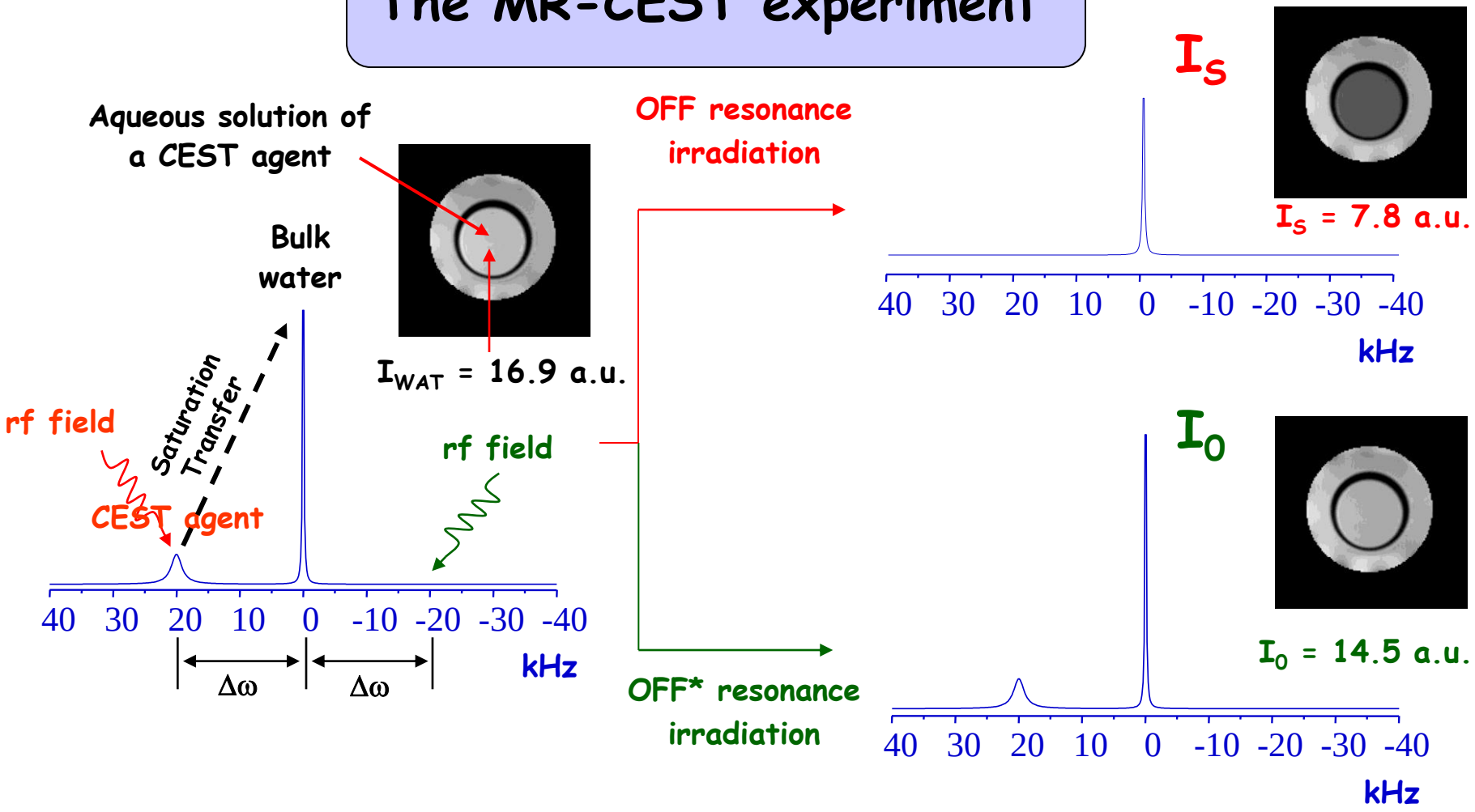

The decrease of I_{WAT} is the source of the MR contrast

The net ST % effect is calculated as $(1 - I_S/I_0) \cdot 100$

CEST agents: the sensitivity issue

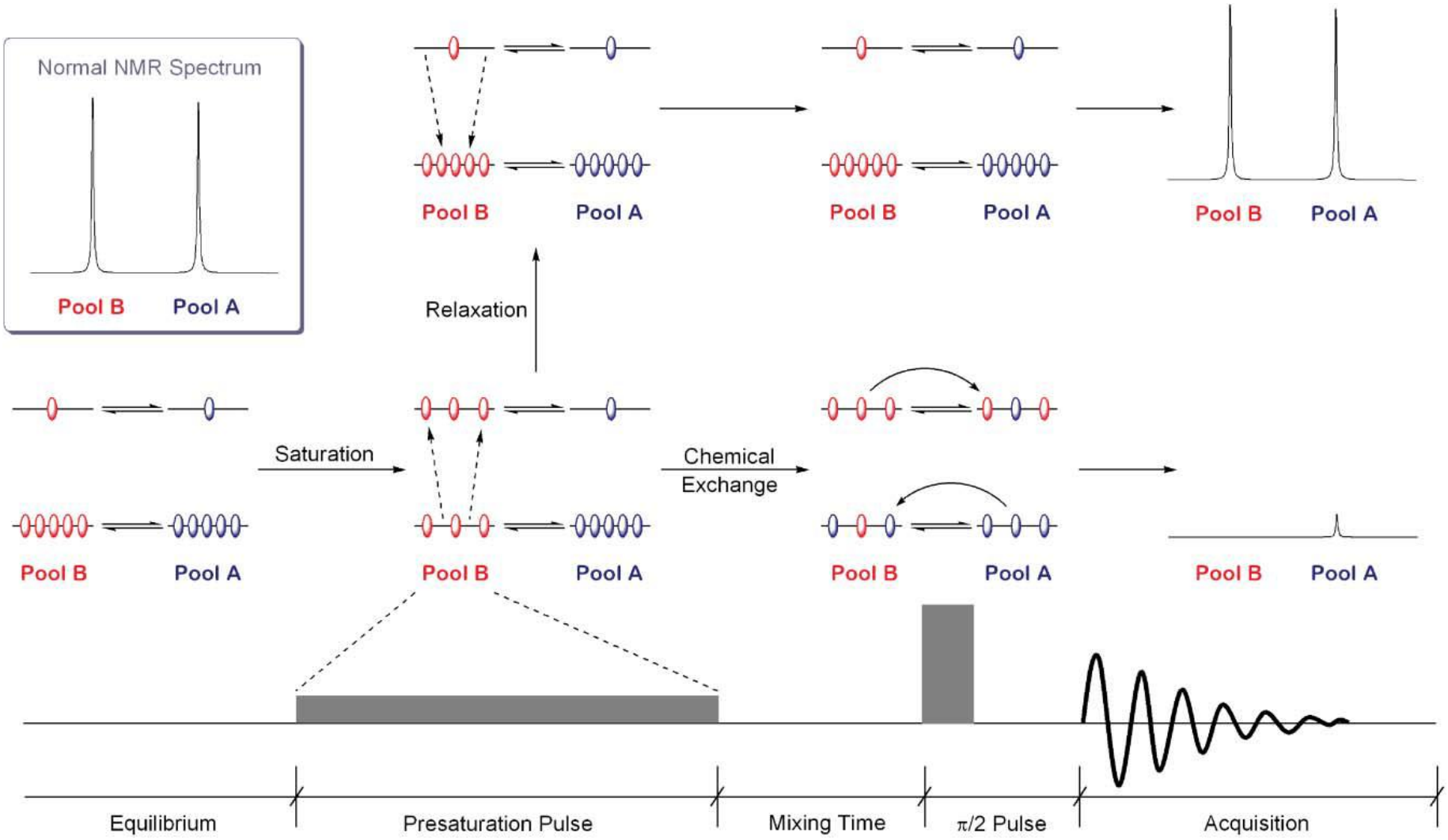

Sherry D. et al.*Chem. Soc. Rev., 2006, 35, 500–511*

$$ST = 1 - \frac{I_S}{I_0} = \frac{k_{ex} f_{CEST}}{R_1^w + k_{ex} f_{CEST}} \left(1 - e^{-t_{sat}\left(R_1^w + k_{ex} f_{CEST}\right)}\right)$$

Where:

$$f_{CEST} = \frac{n[CA]}{2[BulkW]}$$

Exchange rate of the mobile protons belonging to the contrast agent(CA)

Relaxation rate of the bulk water protons

Concentration of the contrast agent

Number of magnetically equivalent mobile protons

Experimental parameter: irradiation time

$$ST = 1 - \frac{I_S}{I_0} = \frac{k_{ex} f_{CEST}}{R_1^w + k_{ex} f_{CEST}} \left(1 - e^{-t_{sat}\left(R_1^w + k_{ex} f_{CEST}\right)}\right)$$

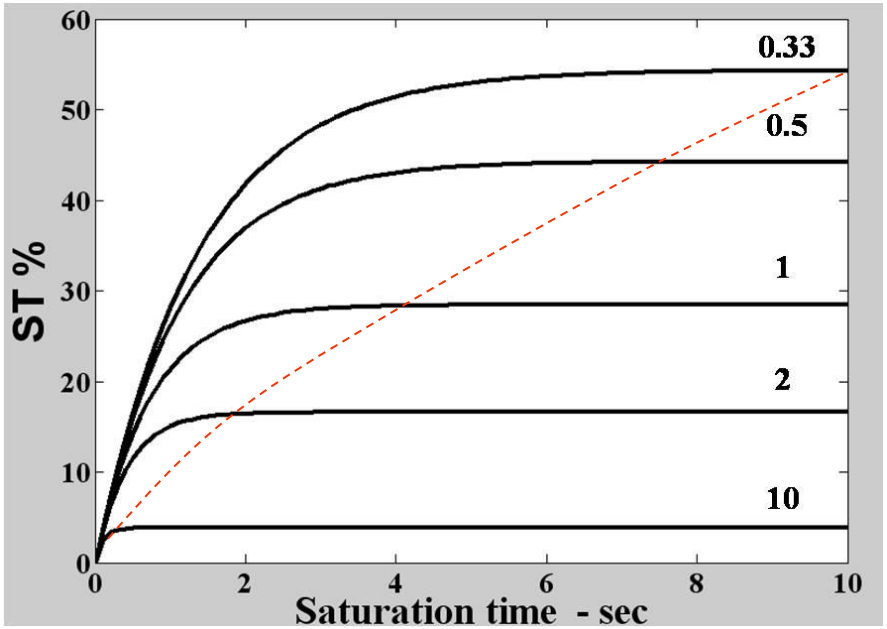

Increase of R_1 bulk water pool

Simulation parameters* $f_{CEST} = 5\times10^{-4}$, $R_2^{bw} = 2\times R_1^{bw}$, $R_1^{CEST} = 2\ s^{-1}$, $R_2^{CEST} = 50\ s^{-1}$, $k^{CEST} = 1600\ s^{-1}$, $B_2 = 6\ \mu T$
Woessner et al, MRM 2005

The steady-state condition is reached when $e^{-\left(R_1^{bw} + k_{ex}^{CEST} f_{CEST}\right)} = 0$

↓

In addition to R_1^{bw}, also an increase of the exchange rate accelerates the achievement of the steady state condition

Sensitivity of CEST agents: playing with k_{ex}

In principle, the CEST efficiency is proportional to k_{ex}, but the exchange rate cannot be increased at will, because:

i) the condition $\Delta\omega > k_{ex}$ has to be satisfied

ii)

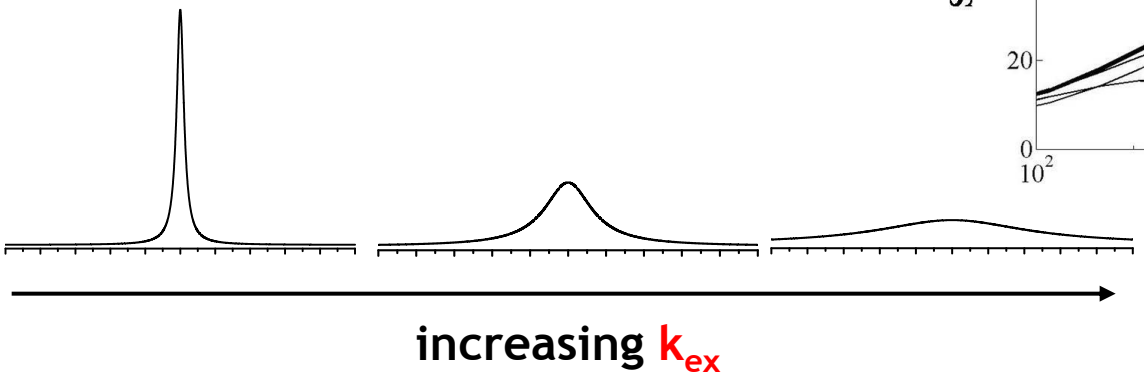

increasing k_{ex}

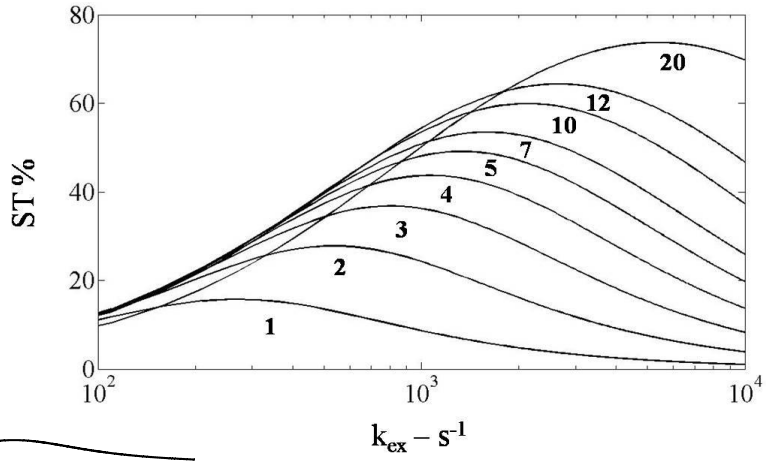

Max. CEST $\frac{k_{ex}}{B_2} = 2\pi$

Fast exchange requires high-intensity saturation fields for achieving full saturation

- overcoming SAR* limitations ➡ unsafe saturation
- direct saturation of bulk water ➡ less efficient CEST contrast

*SAR = Specific Absorption Rate. It is defined as the RF power absorbed per unit of mass of an object, and is measured in watts per kilogram (W/kg).*SAR* of 1 Wkg^{-1} applied for an hour would result in a temperature rise of about 1 °C.

Sensitivity of CEST agents: increasing the number of saturated protons

The CEST efficiency is proportional to the number of mobile protons

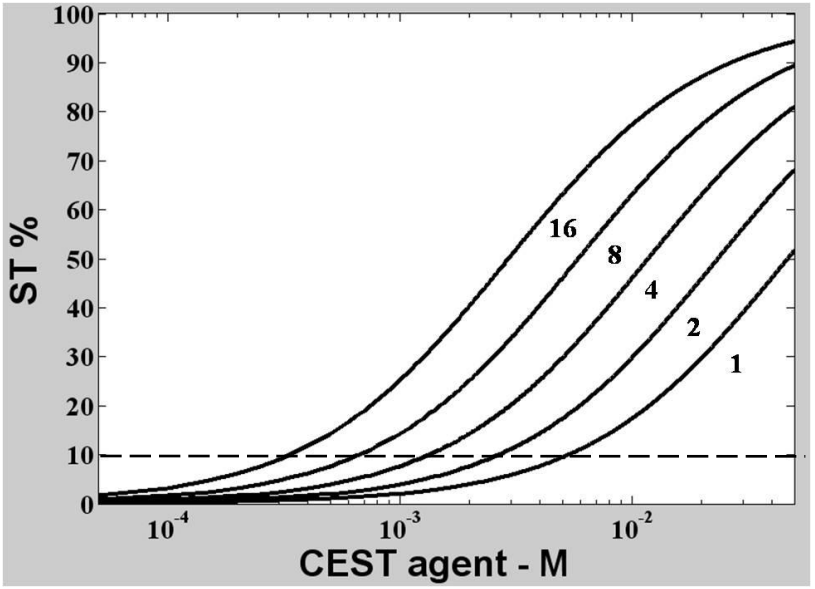

A CEST contrast of 10% requires few millimolar of mobile protons

The sensitivity can be improved by increasing the number of mobile protons (with equal or similar $\Delta\omega$ values) per CEST molecule

Mobile protons	Sensitivity	Chemical system
< 10	mM	Low MW molecules
10^3	μM	Macromolecules
10^6	nM	Nanoparticles

Optimizing the saturation scheme

The overall saturation time can be covered by:

- **a single cw rectangular pulse**

- **a train of shaped pulses**

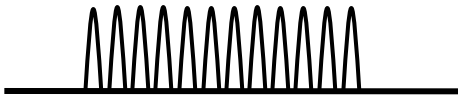

Single cw saturation pulses (2-10 s long) have been observed to be more efficient in case of probes with relatively slow exchange: DIACEST (B_2 1-3 μT), PARACEST (typically amide protons or slowly exchanging Ln-bound water protons, B_2 12-24 μT), and LipoCEST (B_2 6-12 μT)

BUT

Pulsed shaped pulses are definitely better in terms of deposited energy and clinical translation

CEST agents: the sensitivity issue

CEST contrast is quite sensitive because few millimolar of saturated mobile protons are sufficient to affect the MRI signal (> 100 molar)

However, the development of highly sensitive agents is an hot issue, especially for molecular imaging purposes.

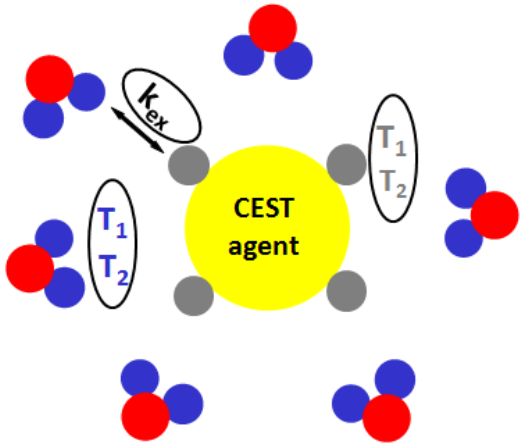

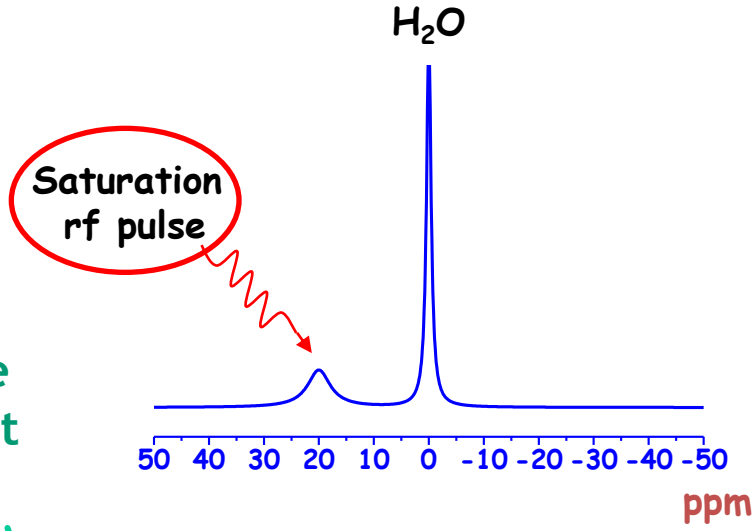

Variables affecting the CEST contrast

- Exchange rate of the CEST protons
- Resonance frequency of the CEST protons
- Total concentration of saturated spins
- T_1 and T_2 of both the exchanging sites

- Duration of saturation time
- Saturation scheme (cw, pulsed)
- Saturation pulse power
- Magnetic field strength (affects $\Delta\omega$)

CEST agents: mechanism of action

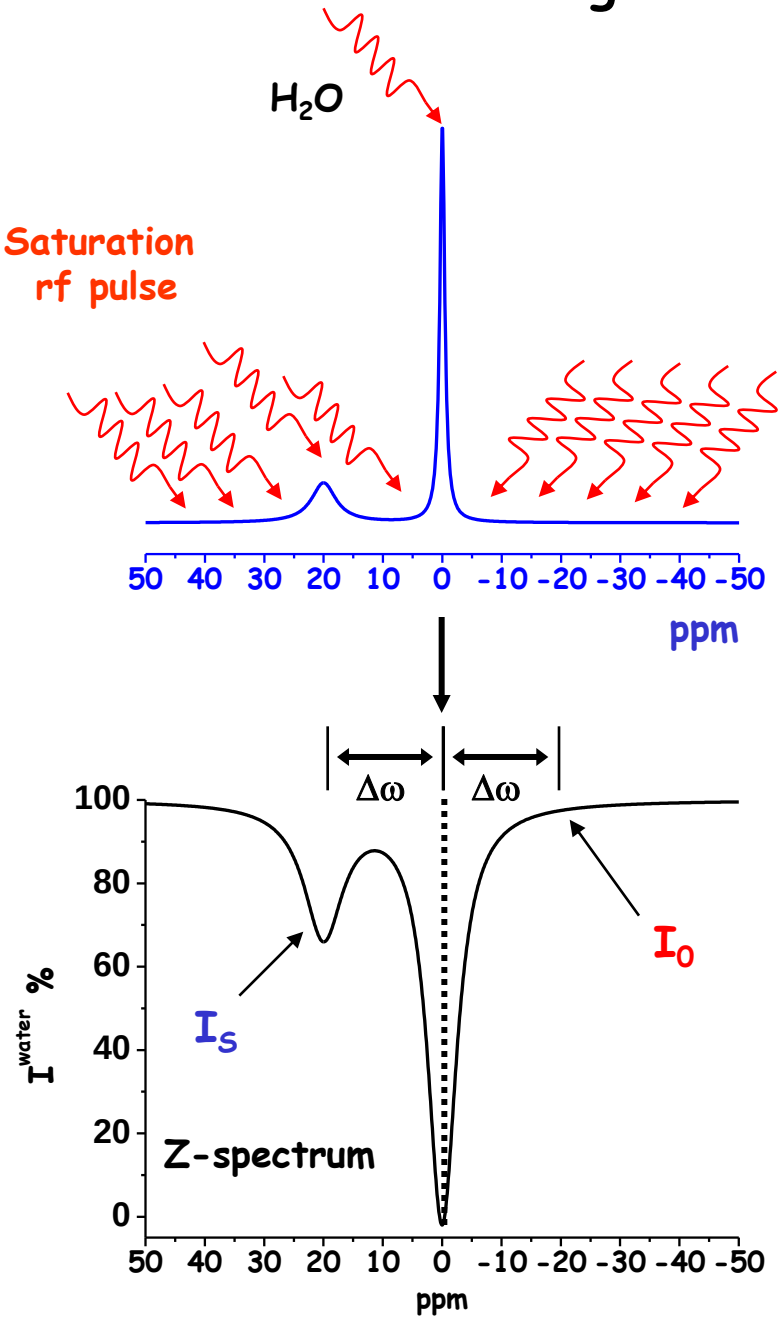

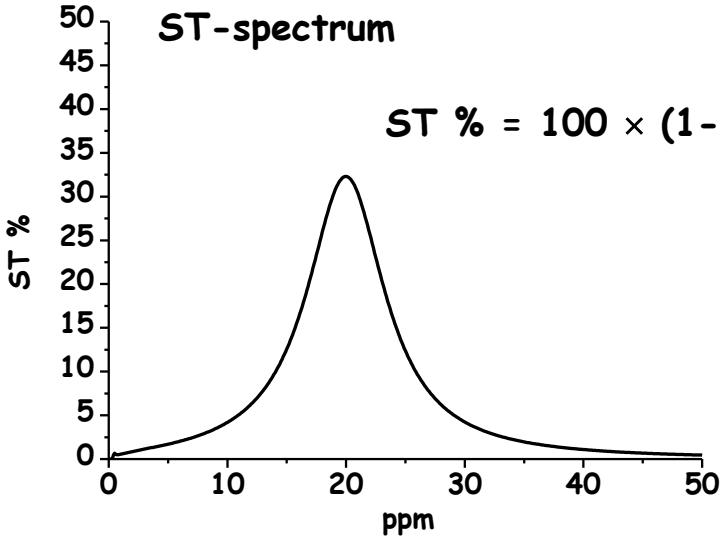

Field homogeneity

B_0 field homogeneity plays a key-role for the detection of CEST contrast, especially in biological specimen

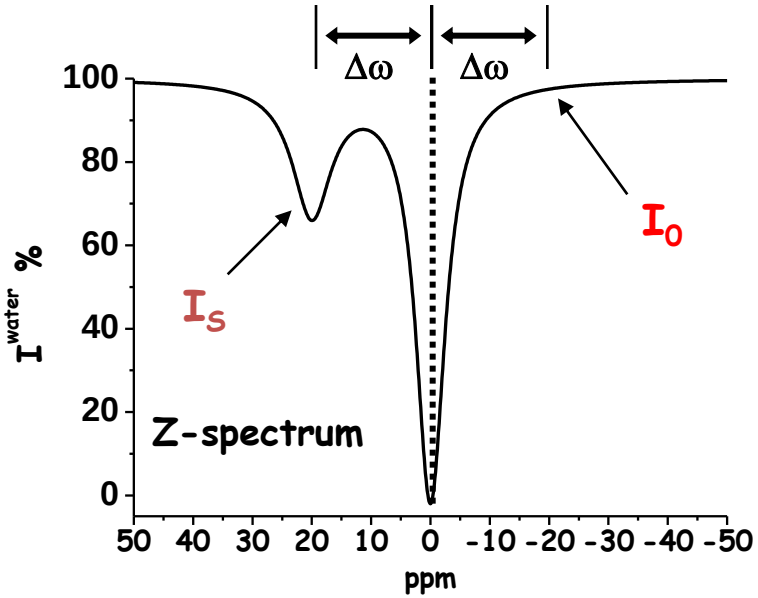

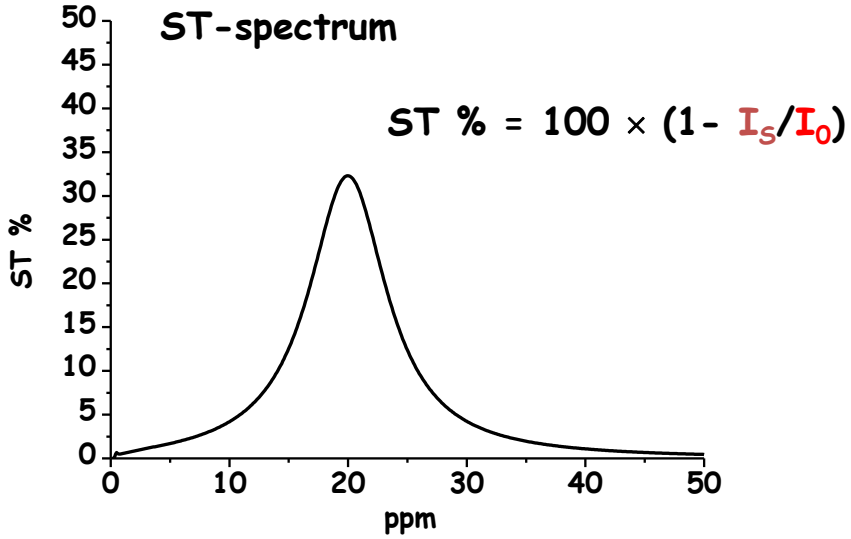

An accurate contrast assessment requires that the two MR signal intensities are measured at frequency offsets symmetrically distributed with respect to the resonance frequency of the bulk water

Field homogeneity

The pixel-by-pixel evaluation of the spatial distribution of the frequency offset of the bulk water is necessary to avoid CEST artifacts…

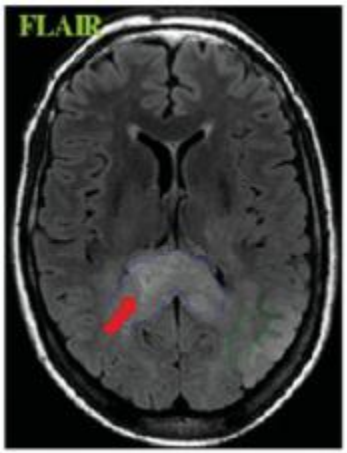

Human astrocytoma

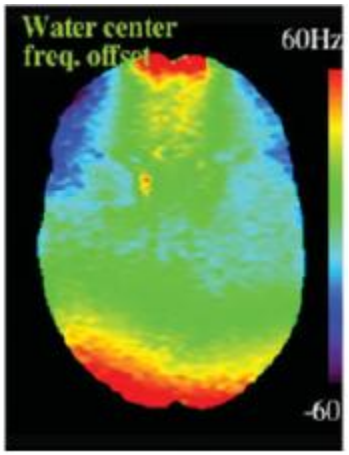

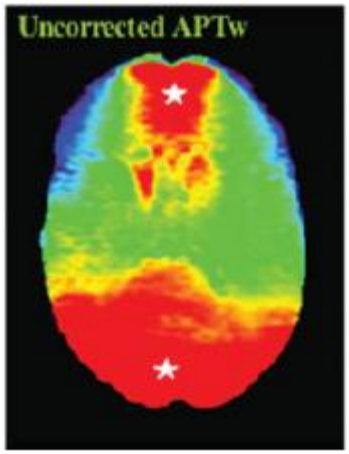

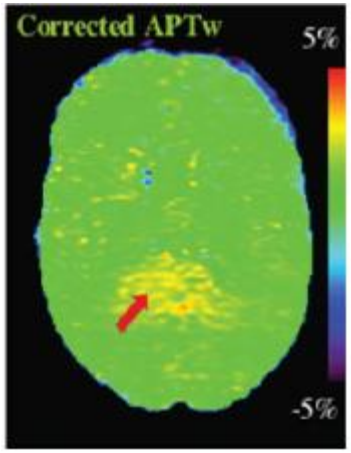

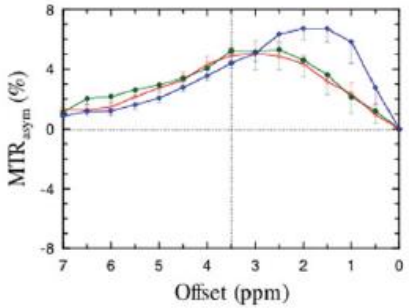

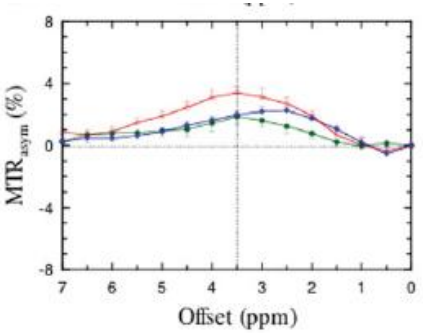

Zhou *et al.*, MRM 2008, 60, 842

Field homogeneity

…but, of course, acquiring B_0 maps takes time

Several methods have been proposed so far:

- **B_0 (and also B_2) compensation algorithm (Sun *et al.*, MRM 2007)**

☺ **relatively fast (in addition to the couple of CEST scans, it requires few images for generating the B_0/B_1 maps)**

☹ **Not suitable for large inhomogeneities**

- **Z-spectrum interpolation (Zhou *et al.*, Nat. Med. 2003 – Stancanello *et al.*, CMMI 2008)**

☺ **broad applicability, good accuracy**

☹ **Relatively time consuming (depending on the frequency sampling)**

- **WAter Saturation Shift Referencing (WASSR) (Kim *et al.*, MRM 2009)**

☺ **excellent accuracy; optimal for detecting CEST contrast from very little shifted agents**

☹ **Time consuming (an additional Z spectrum is required)**

CEST agents vs conventional MRI contrast agents

3D-Gd-MR Angiography

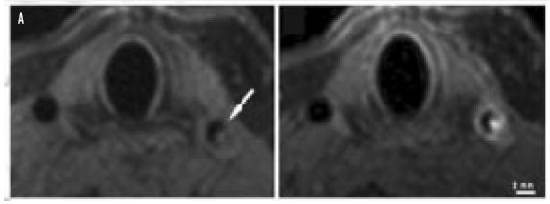

Gd-based fibrin-targeting agent
(visualisation of non-occlusive thrombi)

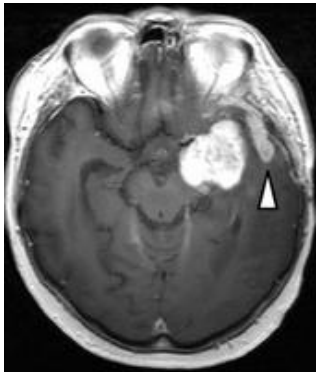

Gd-enhanced MR images
(Glioma)

Do we actually need a new class of MRI agent ?

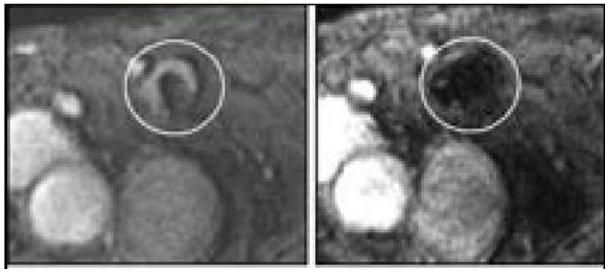

MRI cell tracking experiment
(Limph node targeting by tumor specific SPIO-labeled dendritic cells)

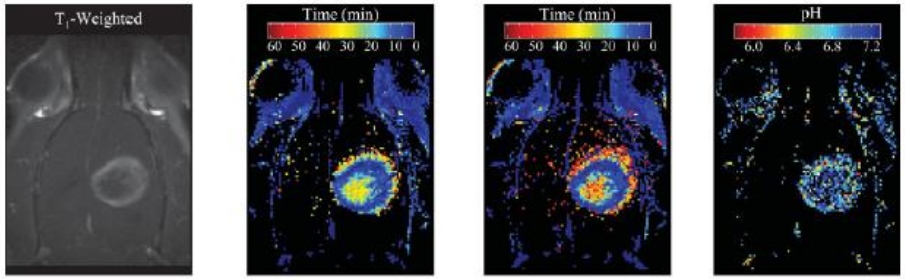

in vivo pH mapping of tumors

Multiple visualization of MRI agents

In vivo **multiple visualization of MRI probes would considerably improve the potential of MRI in many molecular imaging experiments (e.g. multi-detection of epitopes, simultaneous tracking of different cell populations, dynamic measurements,...)**

Example: vivo **Fluorescence image of a lymph node**

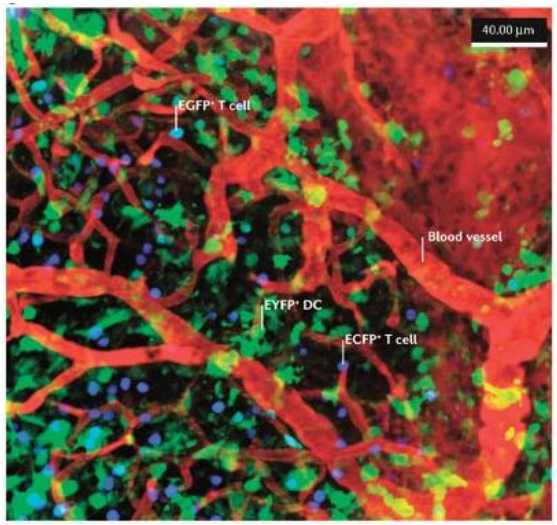

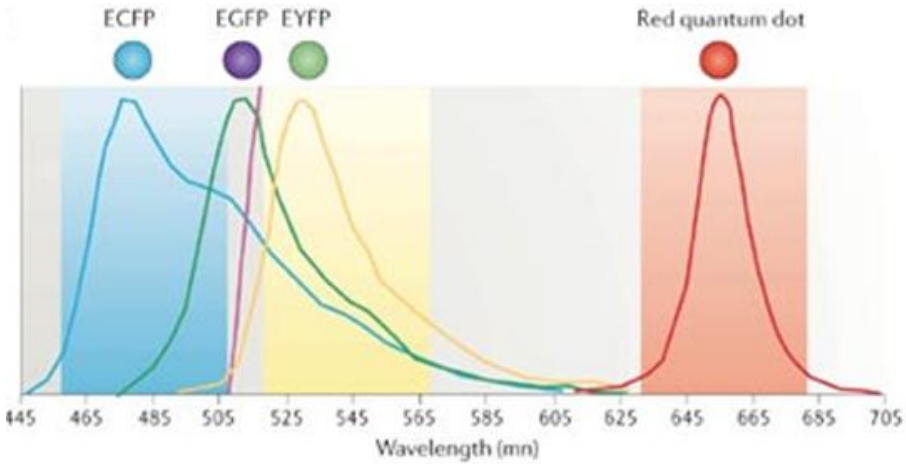

R .N. Germain *et al, Nature Rev. Imm., 2006, 6, 497*

Can we get similar results using MRI agents?

NMR provides a parameter that can characterise any molecule:

the resonance frequency of its spins

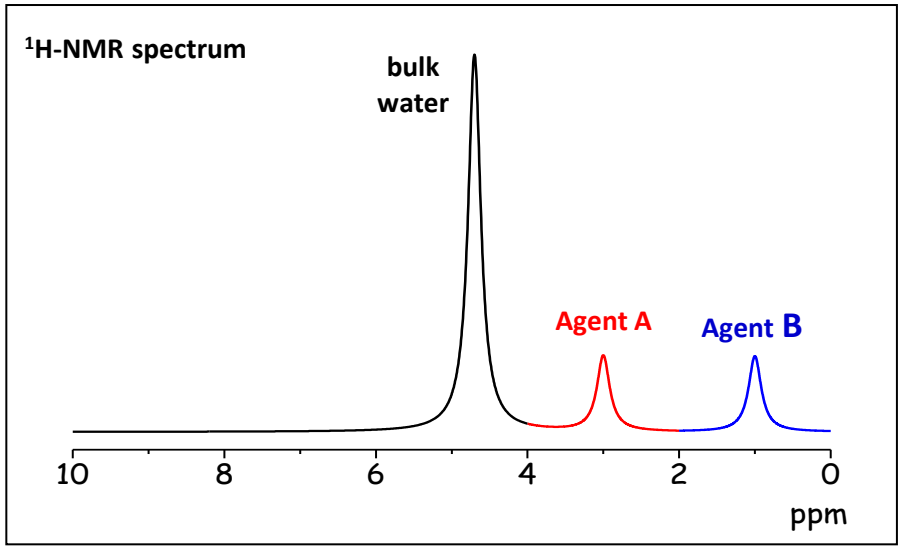

Multiple detection can be achieved by generating a "frequency encoded" contrast

For imaging purposes, this information must be transferred to the intensity of bulk water protons

CEST agents vs conventional MRI agents

MULTIPLE DETECTION

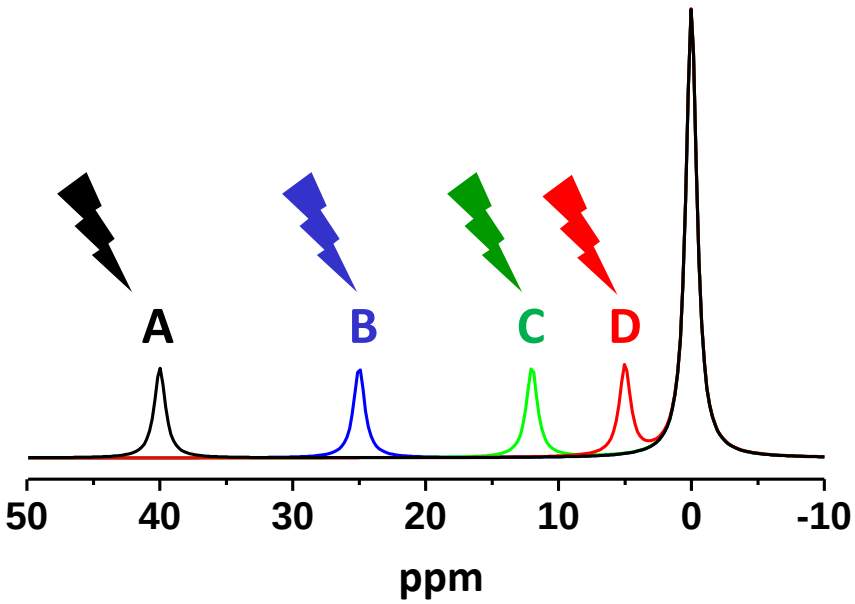

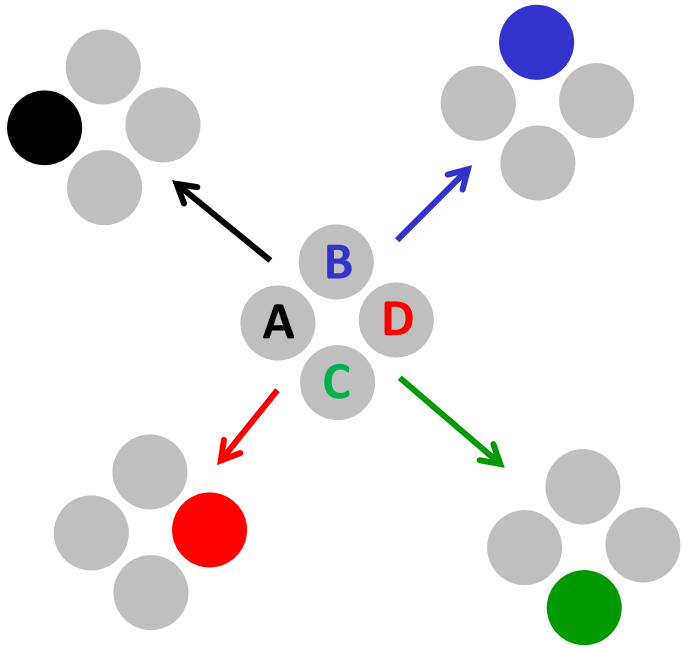

Concentration dependence of the MRI contrast

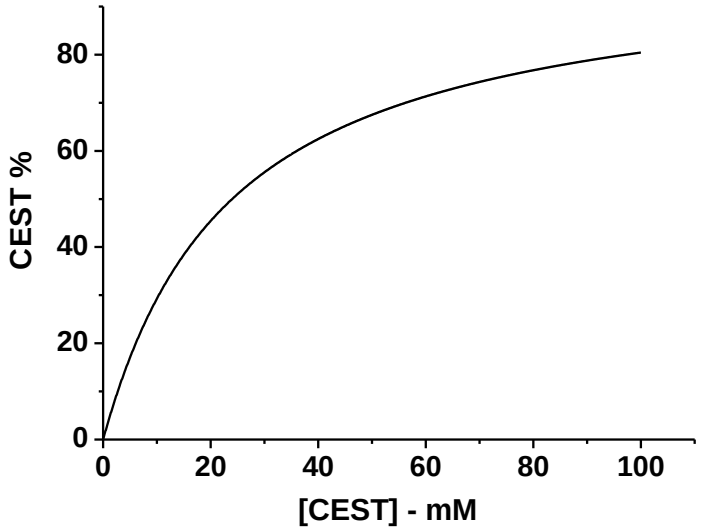

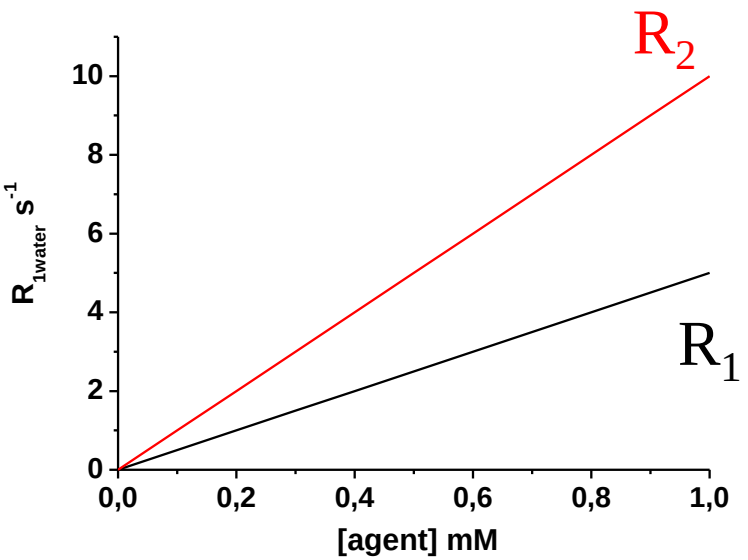

Responsive contrast requires the MRI observable to depend only on the parameter of interest

A ratiometric analysis of the intensity of the water signal after the irradiation of two different mobile pools allows to get rid of the concentration of the MRI probes

CEST agents are very suitable Responsive probes

Ratiometric analysis

$$ST = 1 - \frac{I_S}{I_0} \quad (1); \qquad \frac{I_S}{I_0} = \frac{1}{1 + k_{bw} T_{1w}} \quad (2); \qquad k_{bw} = \frac{k_{ex} n [CA]}{2[BulkW]} \quad (3);$$

by substitution of eq.3 into eq.2 $\longrightarrow$ $$\frac{I_S}{I_0} = \frac{1}{1 + \frac{k_{ex} n [CA]}{2[BulkW]} T_{1w}} \quad (4);$$

$\longrightarrow$ $$\frac{I_0}{I_S} = 1 + \frac{k_{ex} n [CA] T_{1w}}{2[BulkW]} \quad (5); \longrightarrow \frac{I_0}{I_S} - 1 = \frac{k_{ex} n [CA] T_{1w}}{2[BulkW]}$$

If two exchanging pools (A and B) are present in a known ratio (*R*) then...

$$\frac{\left(\frac{I_0}{I_S} - 1\right)^{poolA}}{\left(\frac{I_0}{I_S} - 1\right)^{poolB}} = \frac{\frac{k_{ex}^A n^A [CA]^A \cancel{T_{1w}}}{2[\cancel{BulkW}]}}{\frac{k_{ex}^B n^B [CA]^B \cancel{T_{1w}}}{2[\cancel{BulkW}]}} = \frac{k_{ex}^A n^A [CA]^A}{k_{ex}^B n^B [CA]^B} = \frac{k_{ex}^A}{k_{ex}^B} R$$

Classification of CEST agents

Diamagnetic CEST agents

Paramagnetic CEST agents

Diamagnetic - *vs.* Paramagnetic -CEST agents

$\Delta\omega > k_{ex}$

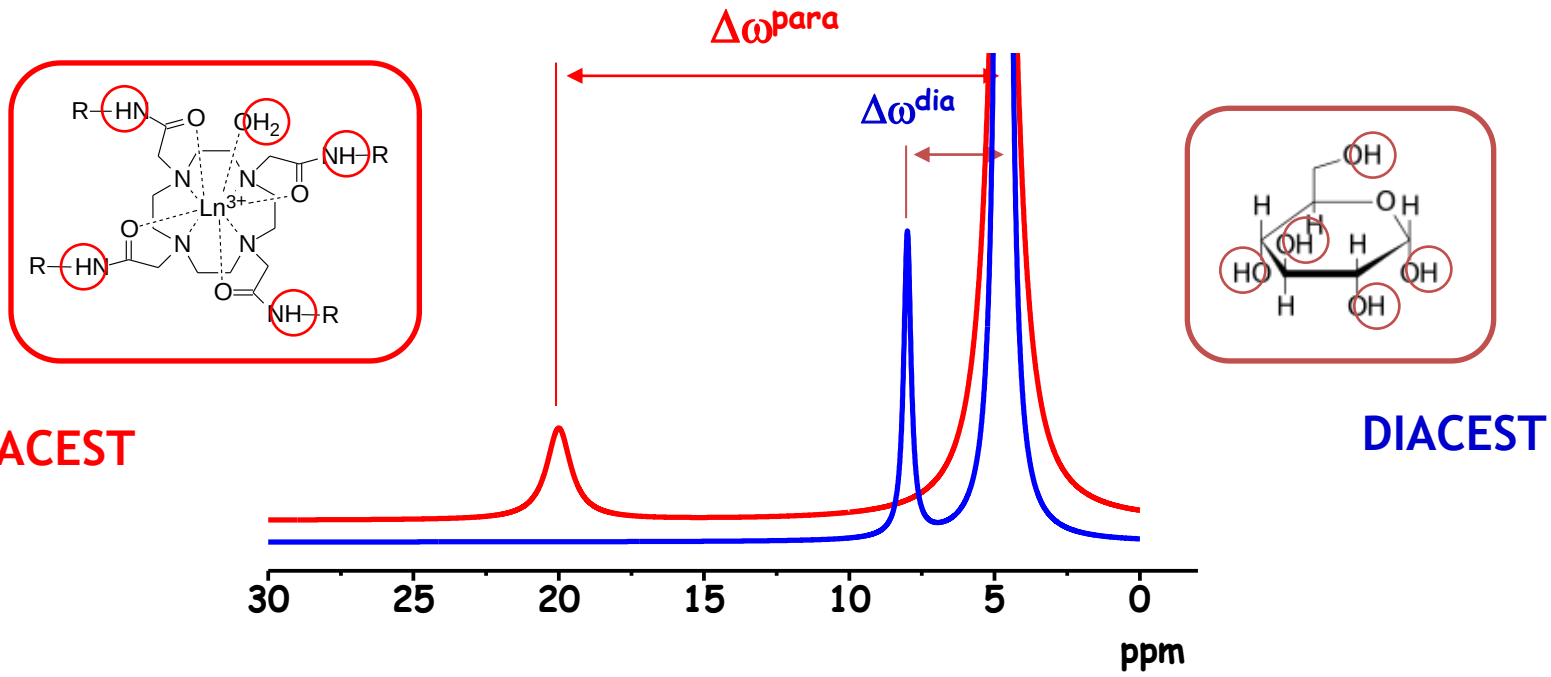

The extension of the $\Delta\omega$ range facilitates multiple visualization and allow to exploit larger exchange rate before coalescence takes place, but the associated line broadening may introduce SAR issues and the T_1 and T_2 shortening may be detrimental for the CEST eficacy

Field homogeneity and highly shifted agents

The detrimental effect of B_0 inhomogeneity progressively vanishes moving away from the resonance of the bulk water

mouse bearing a
B16 melanoma xenograft

(B_2 6 μT)

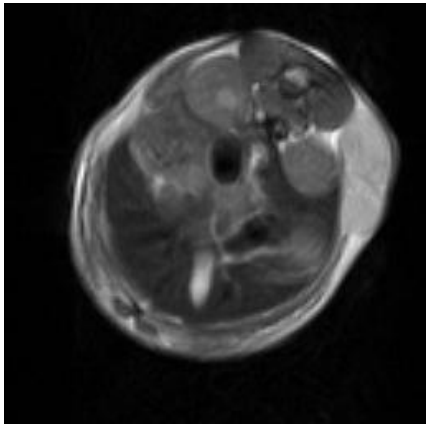

Morphological T_{2w}- image

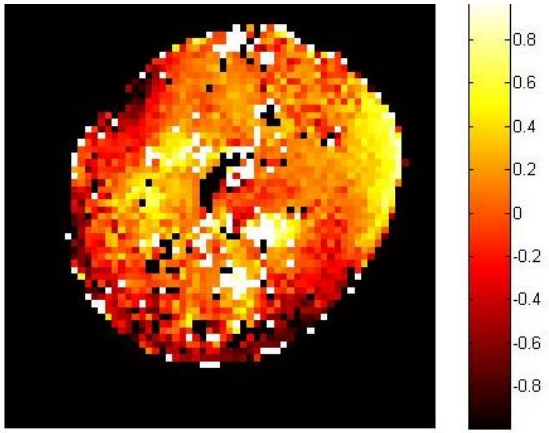

Water shift map

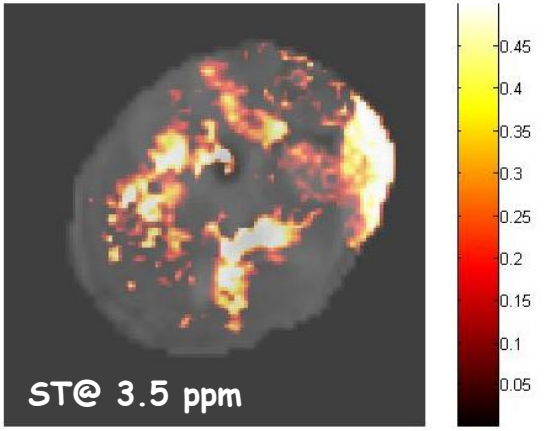

Uncorrected CEST maps

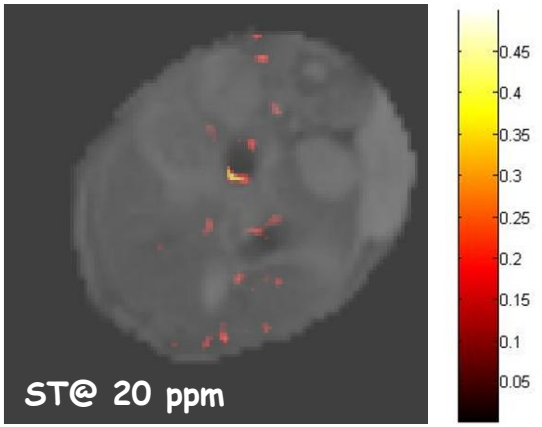

Highly shifted CEST agents can be accurately detected by a simple two scans experiments

Classification of CEST agents

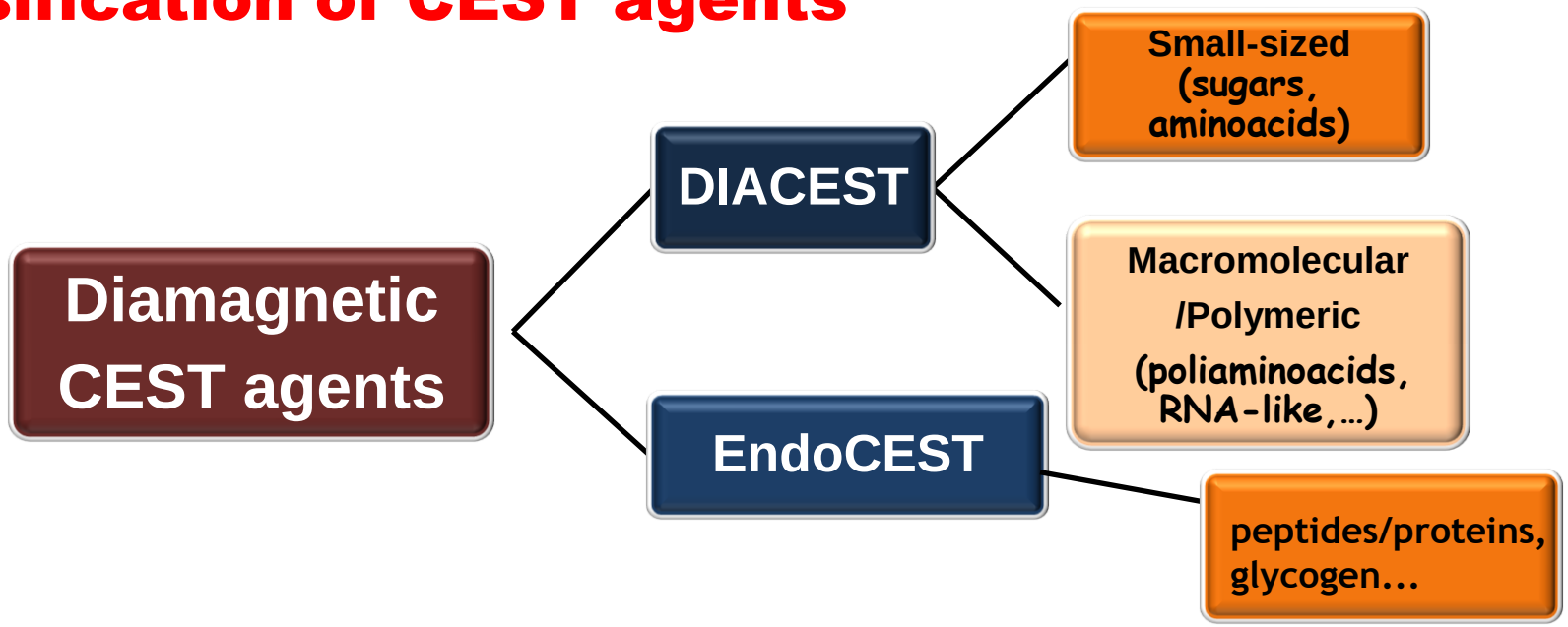

Paramagnetic CEST agents

Endogenous CEST agents (2): APT imaging

Magnetic Resonance in Medicine 56:585–592 (2006)

Amide Proton Transfer Imaging of Human Brain Tumors at 3T

Craig K. Jones,[1,2] Michael J. Schlosser,[3] Peter C.M. van Zijl,[1,2] Martin G. Pomper,[2] Xavier Golay,[1,2,4] and Jinyuan Zhou[1,2*]

Human patient with a meningioma (3 T)

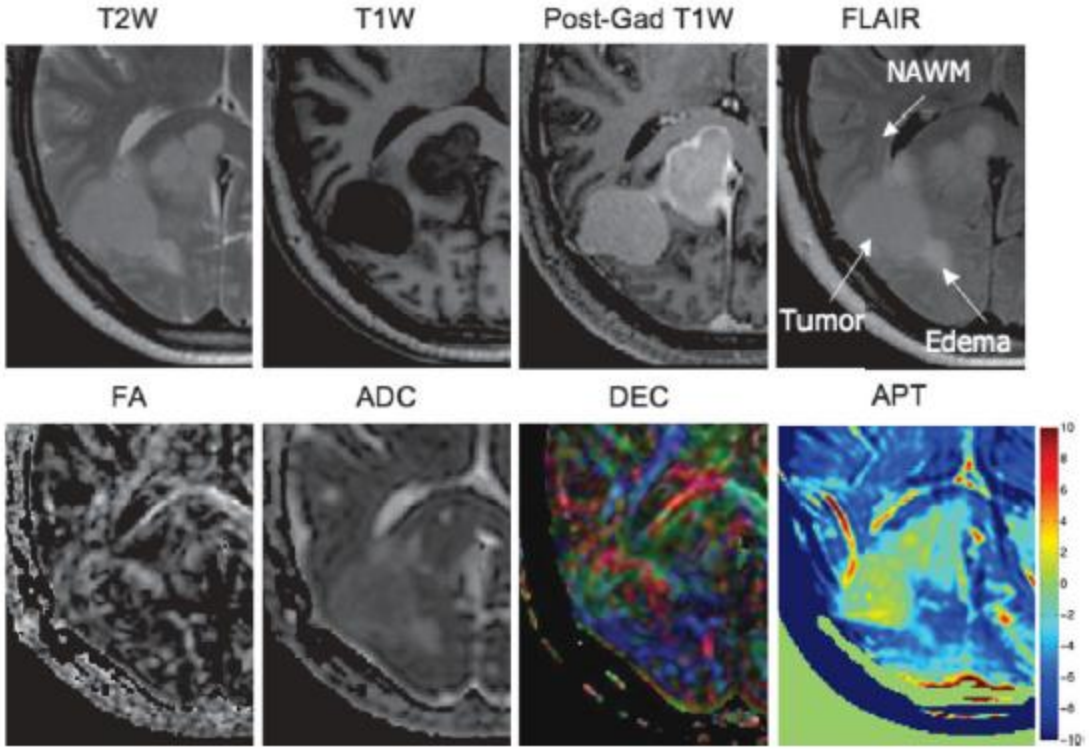

APT imaging may help to discriminate between tumor and edema

Endogenous CEST agents (4): gagCEST

Assessment of glycosaminoglycan concentration *in vivo* by chemical exchange-dependent saturation transfer (gagCEST)

Wen Ling*†, Ravinder R. Regatte‡, Gil Navon†, and Alexej Jerschow*§

2266–2270 | PNAS | February 19, 2008 | vol. 105 | no. 7

In vitro

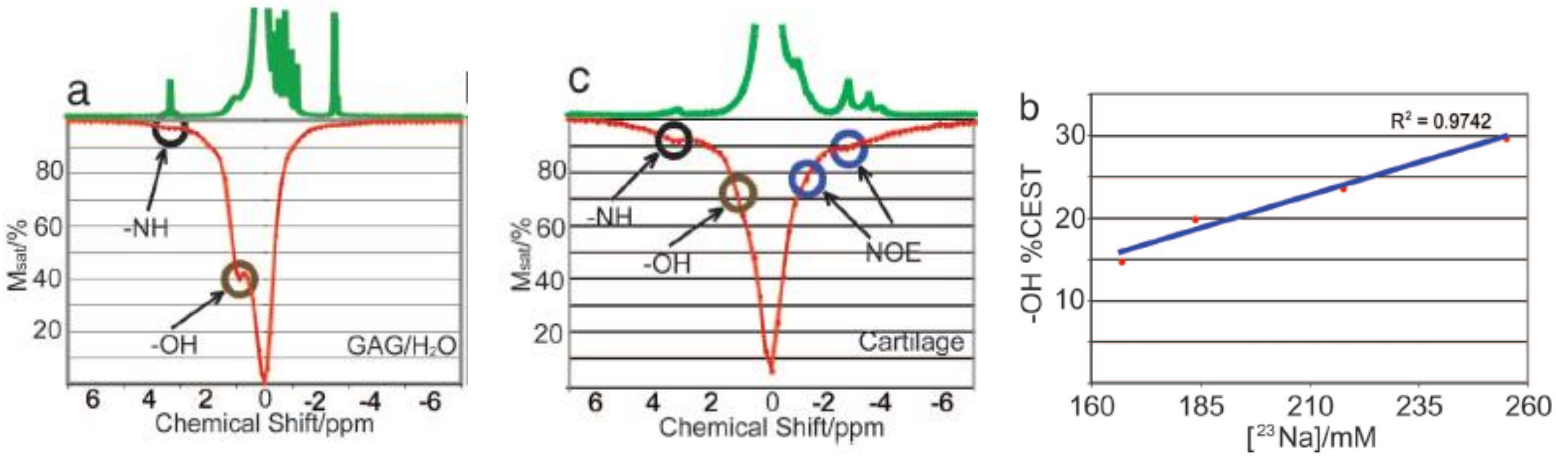

cartilage depletion by tripsine

***In vivo* CEST-MR images of a human patella**

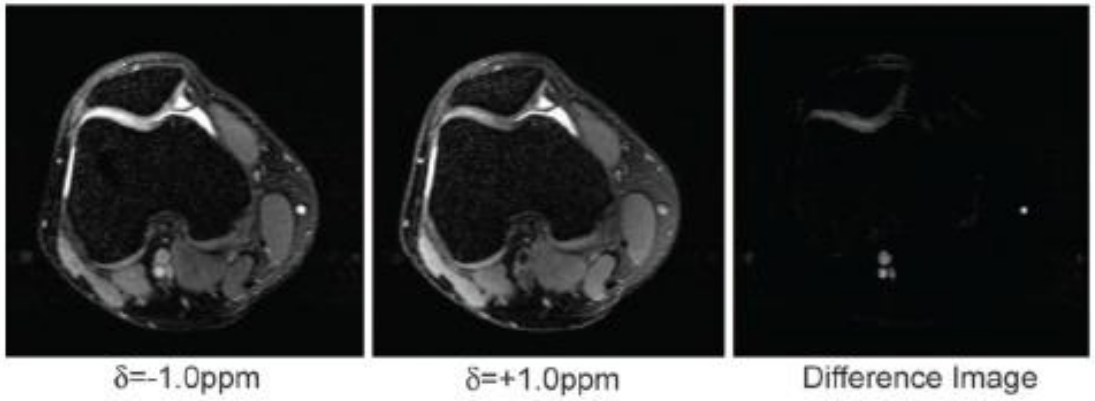

Classification of CEST agents

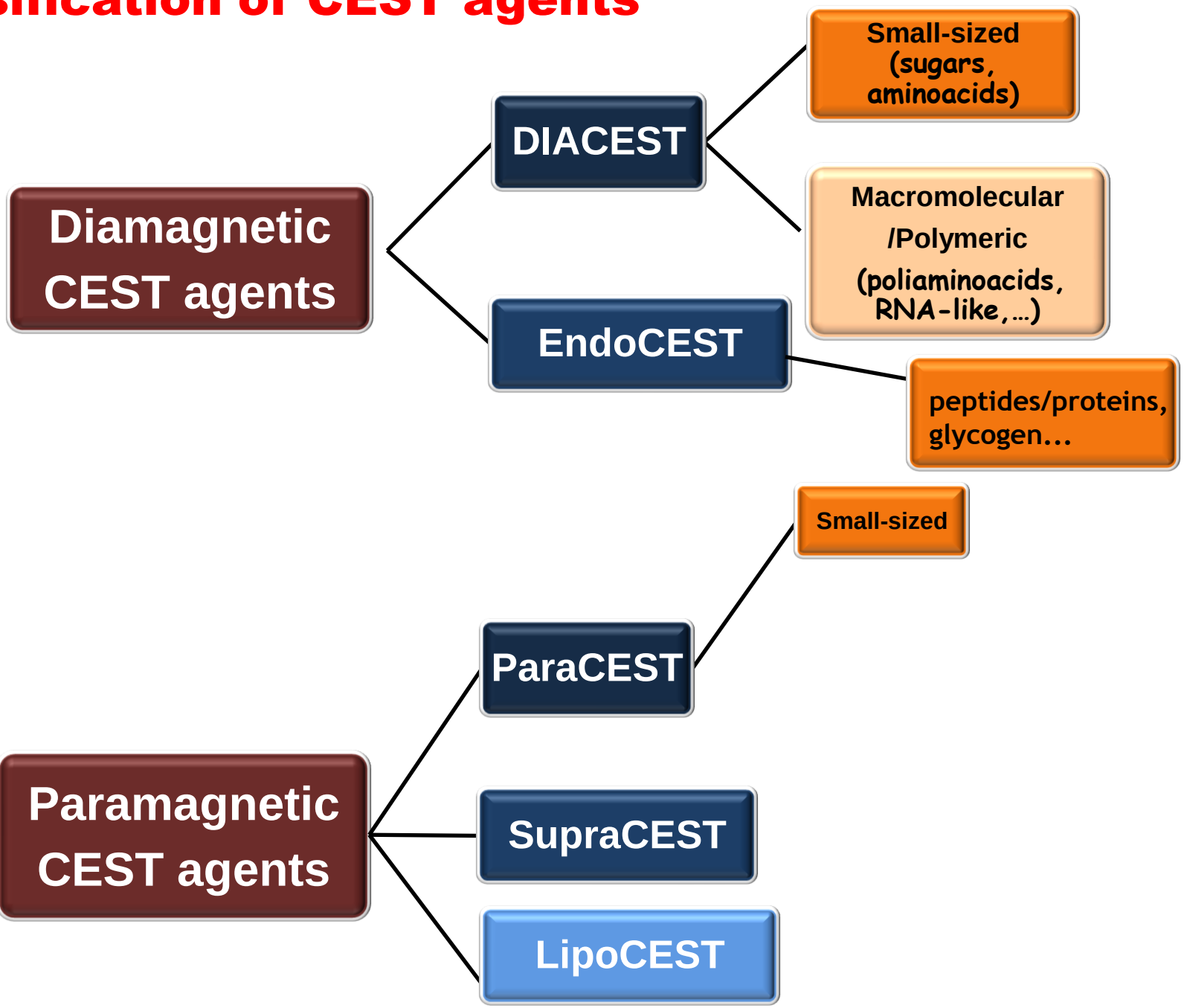

A Novel Europium(III)-Based MRI Contrast Agent

Shanrong Zhang,[†] Patrick Winter,[‡] Kuangcong Wu,[†] and A. Dean Sherry*[,†,‡]

J. Am. Chem. Soc. **2001,** *123,* 1517−1518

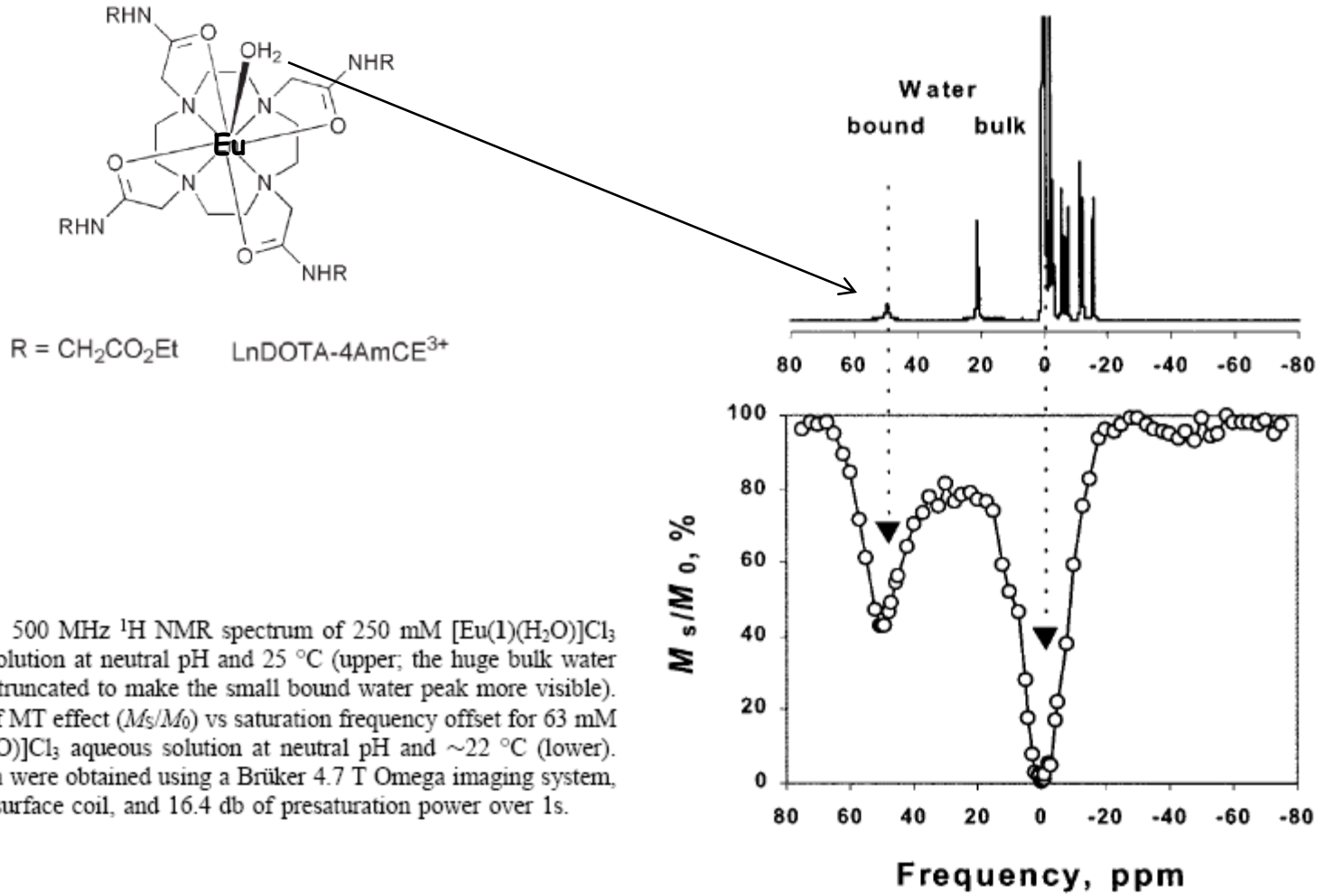

Figure 1. 500 MHz ^{1}H NMR spectrum of 250 mM [Eu(**1**)(H_2O)]Cl_3 aqueous solution at neutral pH and 25 °C (upper; the huge bulk water peak was truncated to make the small bound water peak more visible). A curve of MT effect (M_S/M_0) vs saturation frequency offset for 63 mM [Eu(**1**)(H_2O)]Cl_3 aqueous solution at neutral pH and ~22 °C (lower). These data were obtained using a Brüker 4.7 T Omega imaging system, a 2.5 cm surface coil, and 16.4 db of presaturation power over 1s.

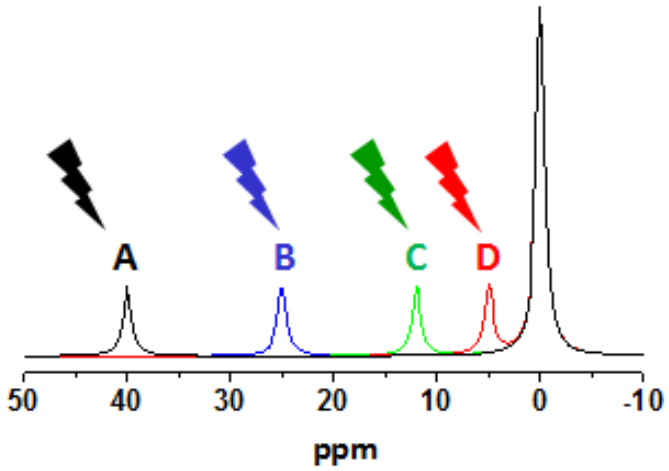

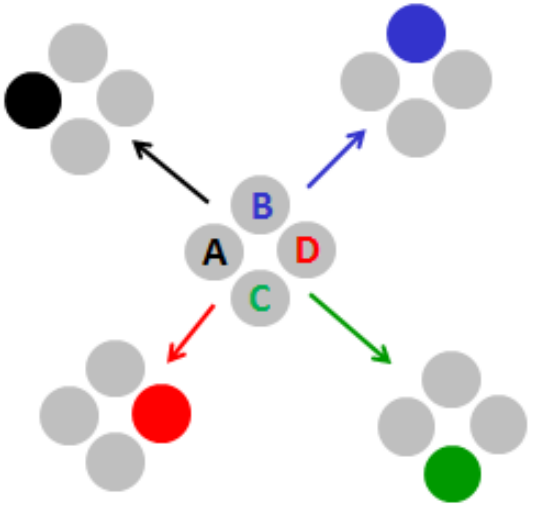

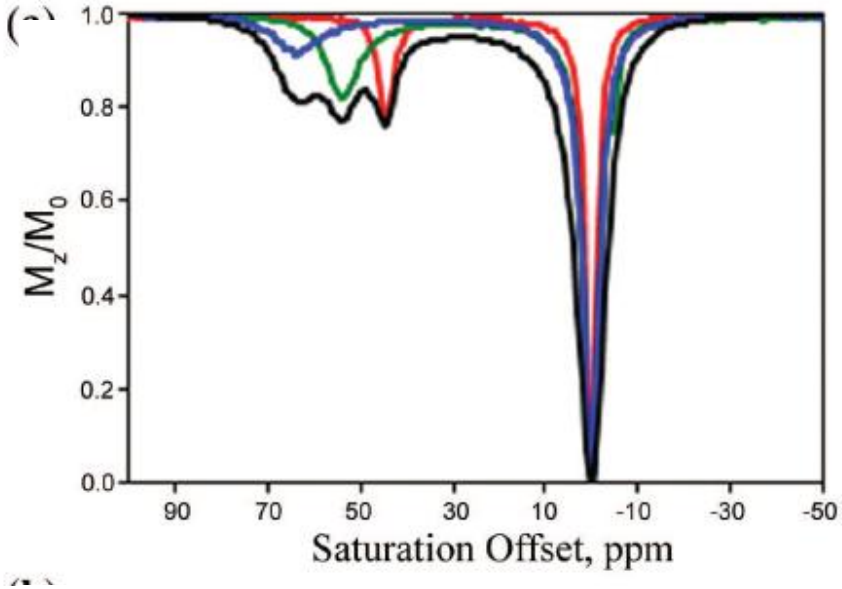

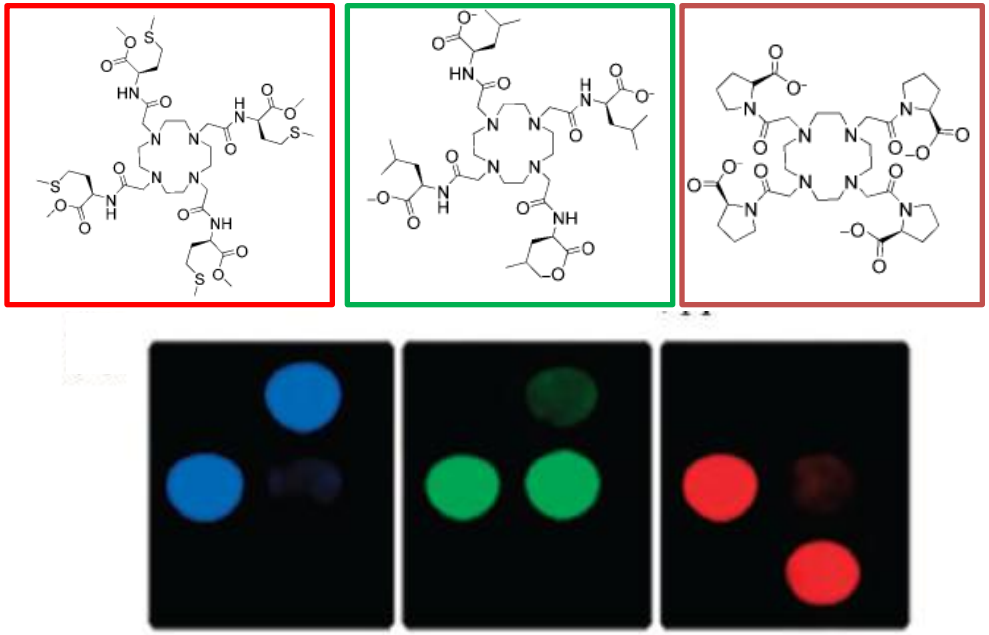

*Subha Viswanathan, S. James Ratnakar, Kayla N. Green, Zoltan Kovacs, Luis M. De León-Rodríguez, and A. Dean Sherry**

Angew. Chem. Int. Ed. **2009**, *48*, 9330–9333

CEST agents for cell-labeling experiments (1)

CEST agents can be used to label different cell populations

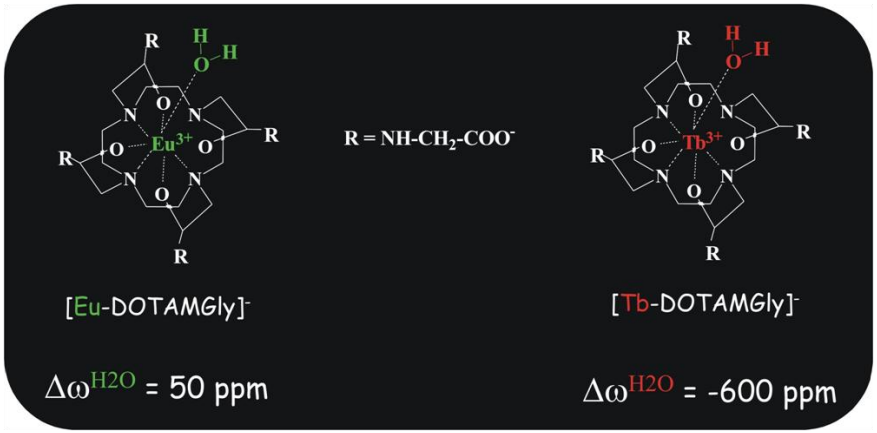

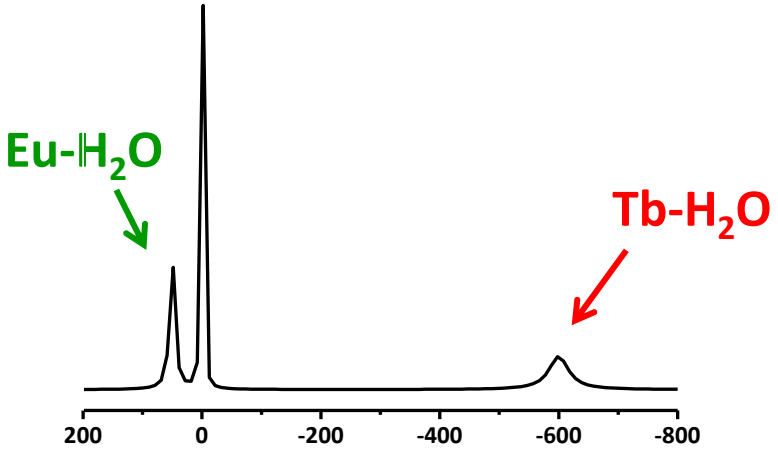

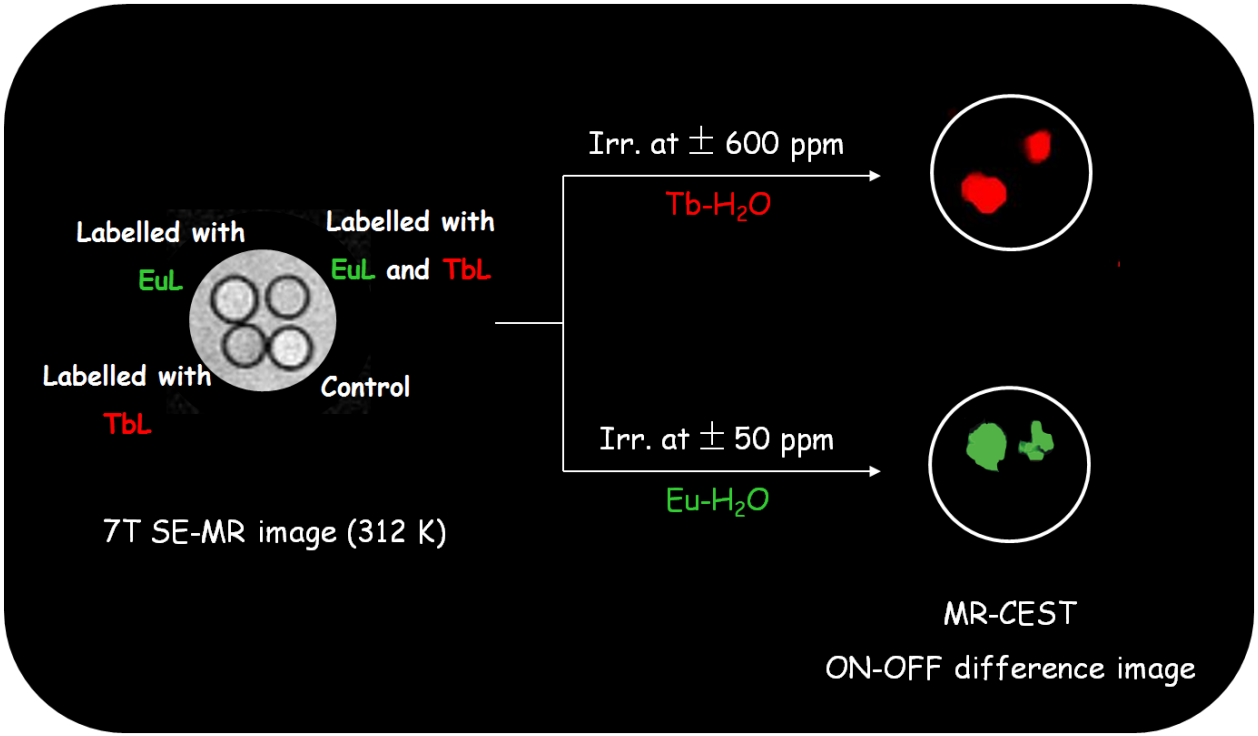

Angew. Chem. Int. Ed. 2005, 44, 1813

Classification of CEST agents

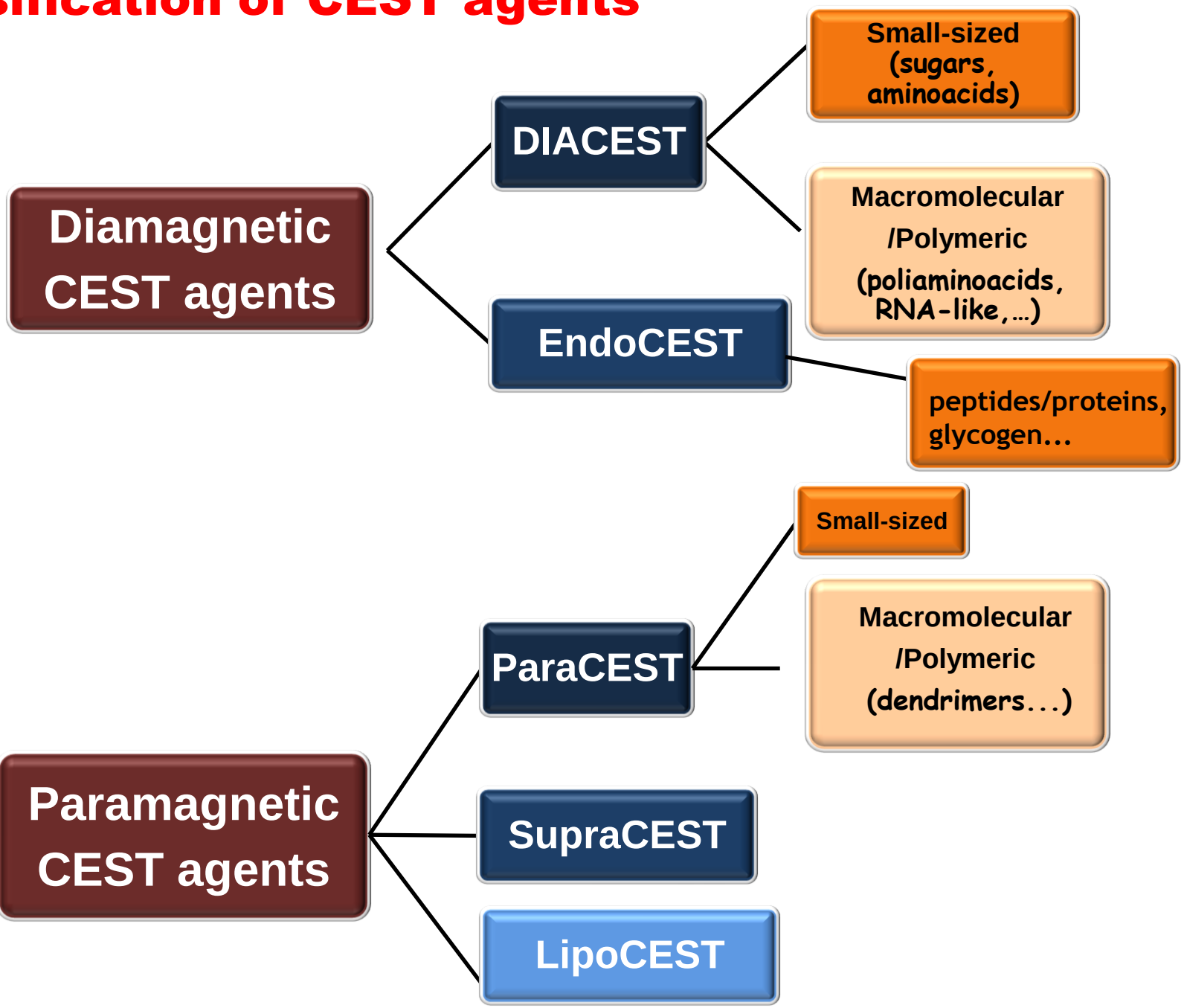

CEST agents for assessing tumor vascular permeability

Simultaneous injection of two agents with different size

Yb-G2

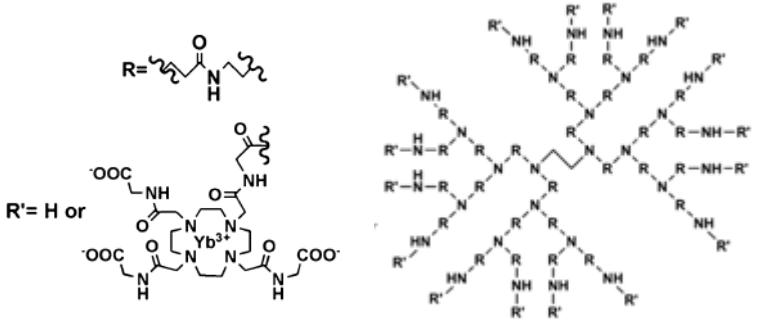

Eu-G5

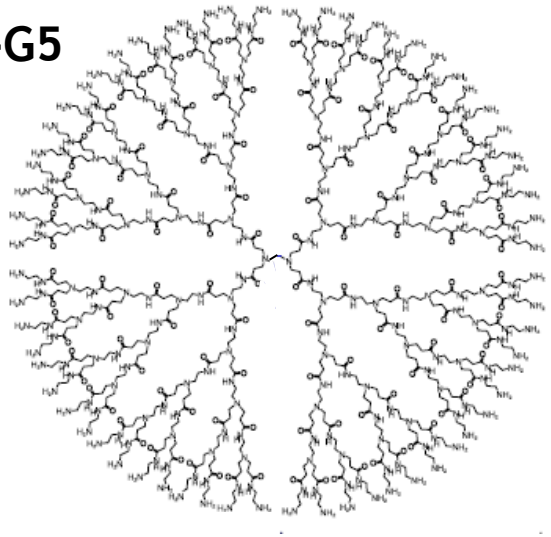

PARACEST agent	concentration to generate a 3.0% PARACEST effect: per lanthanide ion basis	per molecule basis
Eu-DOTA-Gly	1.62 mM	1.62 mM
Eu-G5	1.85 mM	0.045 mM
Yb-DOTA-Gly	1.43 mM	1.43 mM
Yb-G2	1.38 mM	0.242 mM

MCF-7 xenograft tumor on mice

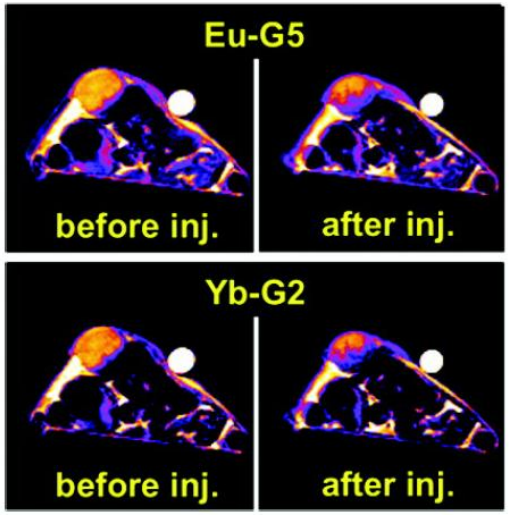

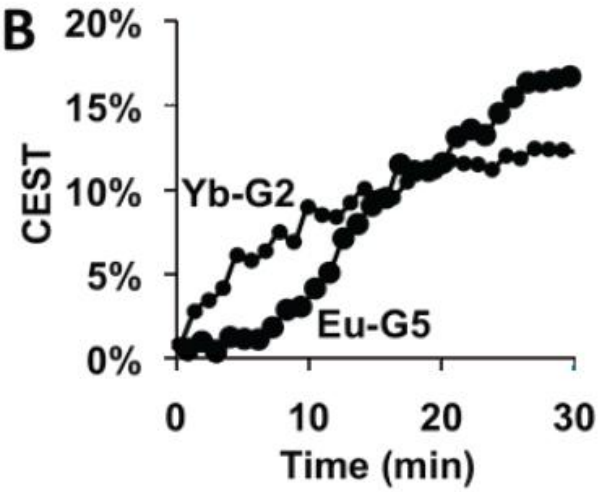

Meser Ali et al., Mol. Pharm. 2009, 6, 1409

Classification of CEST agents

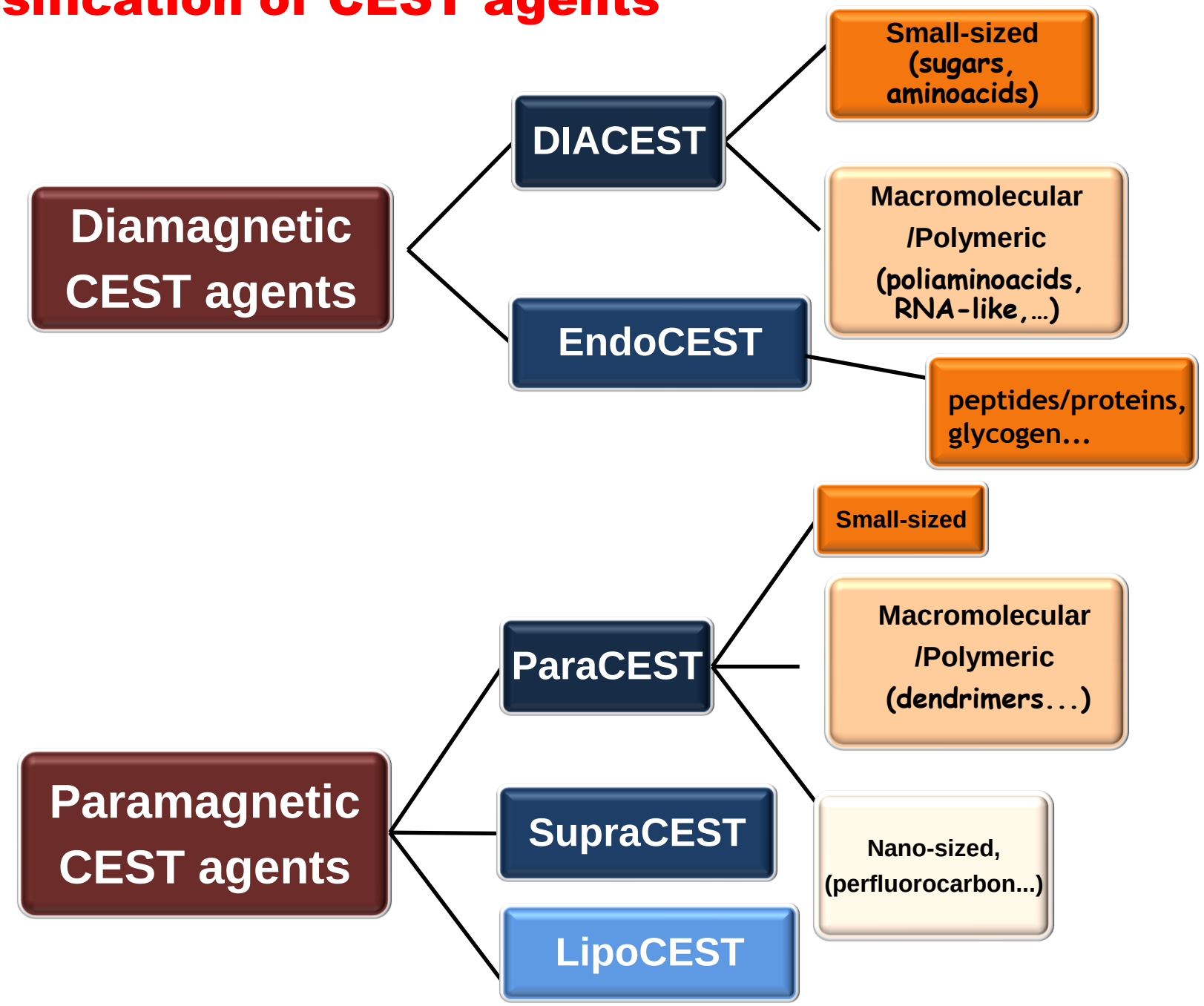

The route to high sensitivity: exploiting nanotechnology

Usually, the typical approach consists of loading a large number of CEST agents to the external surface of the nanosystem:

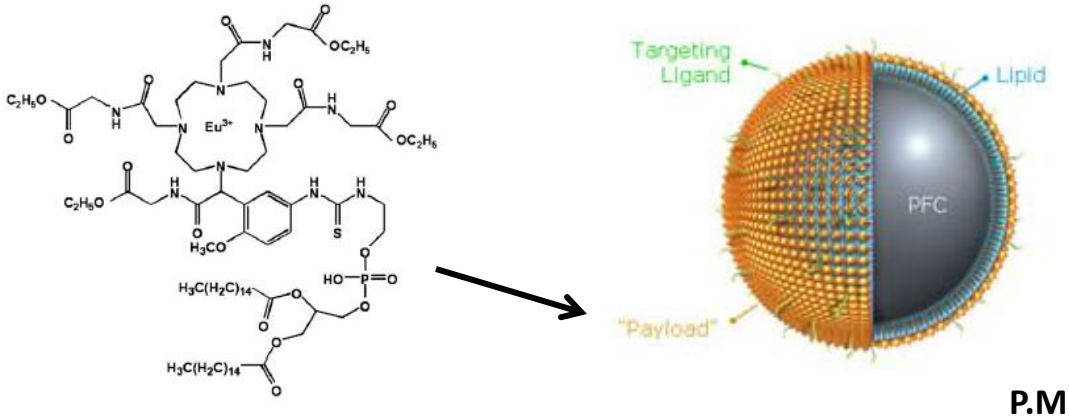

Perfluorocarbon nanoemulsions

P.M. Winter et al. *Mag. Reson. Med.*, 2006, 56, 1384

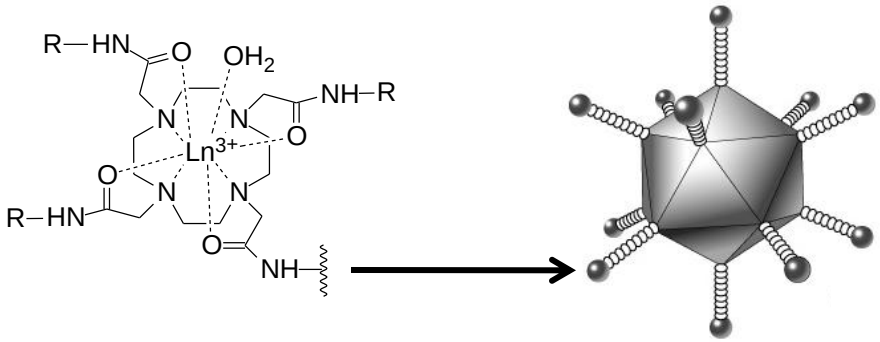

Adenovirus

O. Vasalatiy et al. *Bioconjugate Chem.*, 2008, 19, 598

The sensitivity of such nanoprobes is primarily dependent on the maximum payload that can be achieved (generally 10^3-10^5 PARACEST units per nanosystem)

Macromolecular Paramagnetic CEST agents

To exploit the reversible interaction between a paramagnetic Shift Reagent and a substrate rich of mobile protons

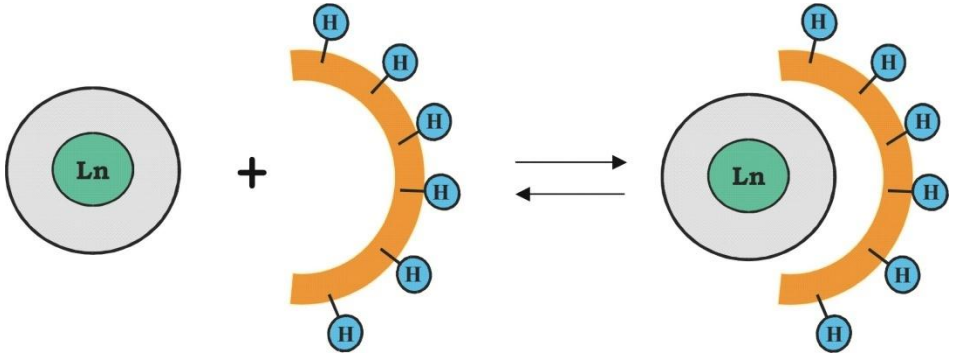

SUPRACEST

Example:

Interaction between

$[TmDOTP]^{5-}$

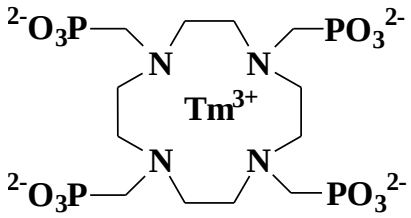

and polyArginine

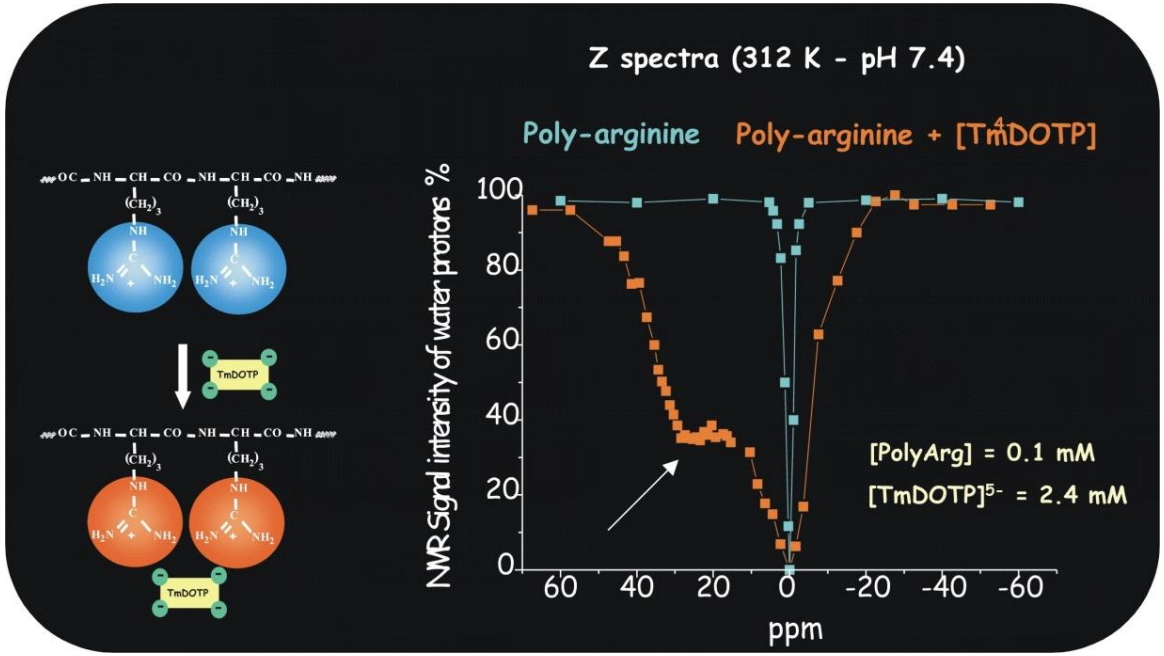

Sensitivity threshold (referred to the paramagnetic complex) of tens of μmolar

S. Aime et al., *Angew. Chemie Int. Ed.*, 2003, 42, 4527

1) **Small-sized molecules** → small number of mobile protons (<10) per molecule

	Sensitivity	B_1 field intensity
a) Diamagnetic agents (sugars, aminoacids,…)	tens of mM	☺
b) Paramagnetic agents		
PARACEST – Amide, hydroxilic protons	few mM	☺
PARACEST – metal bound water protons	hundreds of μM	☹

2) **Macromolecular agents** → large number of mobile protons (~10^3) per molecule

a) Diamagnetic agents (poliaminoacids, RNA-like,…)	μM	☺
b) Paramagnetic agents		
SUPRACEST agents	few μM	☹

3) **Nanoparticles** → extremely high number of mobile protons (>10^6) per molecule

LIPOCEST agents	tens of pM	☺

Liposomes

Biocompatibles, extremely versatiles, successfully used in pharmaceutical field

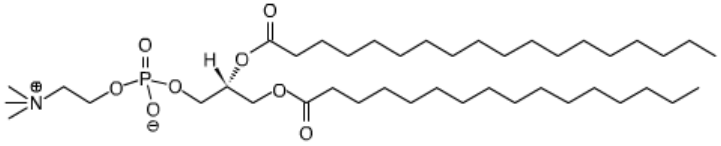

DPPC: DiPalmitoyl-PhosphatidylCholine

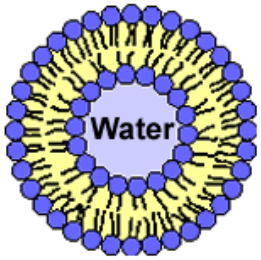

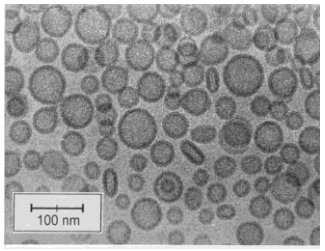

Cryo-TEM image

➢ **The external surface may be easily functionalized with a wide variety of chemicals including targeting vectors, or PEG chains for prolonging the blood half lifetime (Stealth® liposomes).**

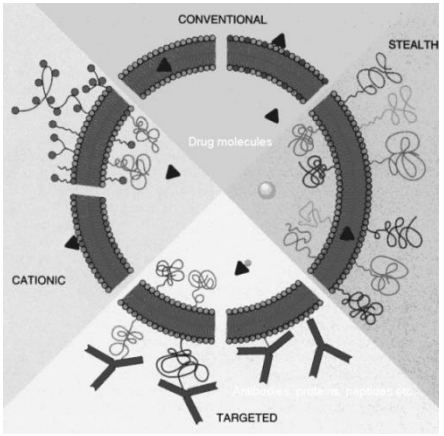

➢ **Liposomes can be passively accumulated in pathological body regions (tumors, atherosclerotic plaques,…)**

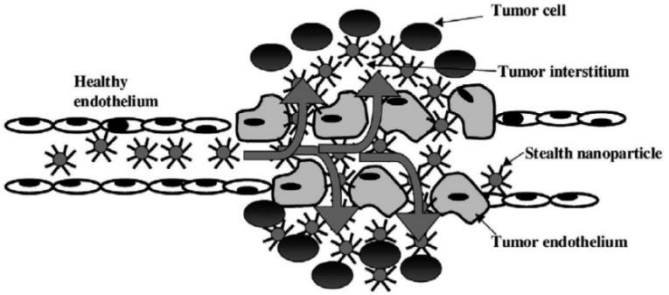

The ST efficiency ∝ to k_{ex} and number of mobile protons

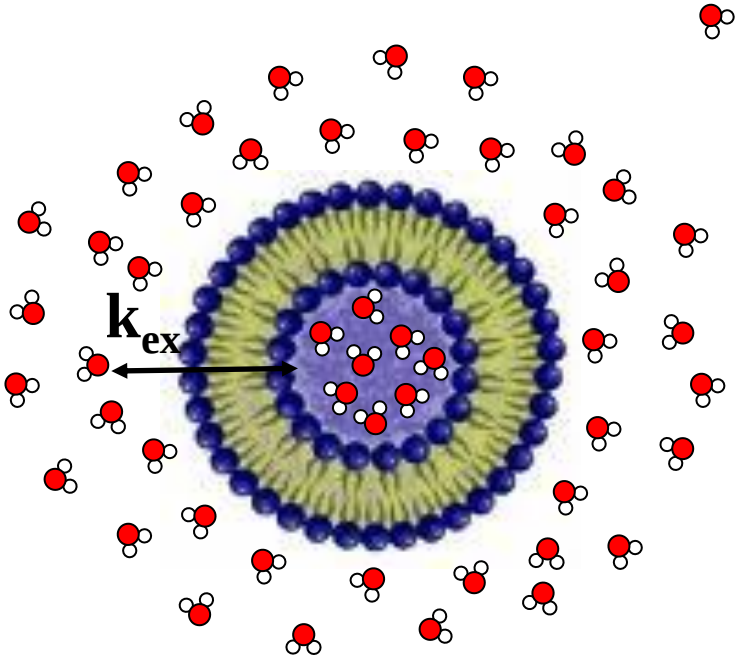

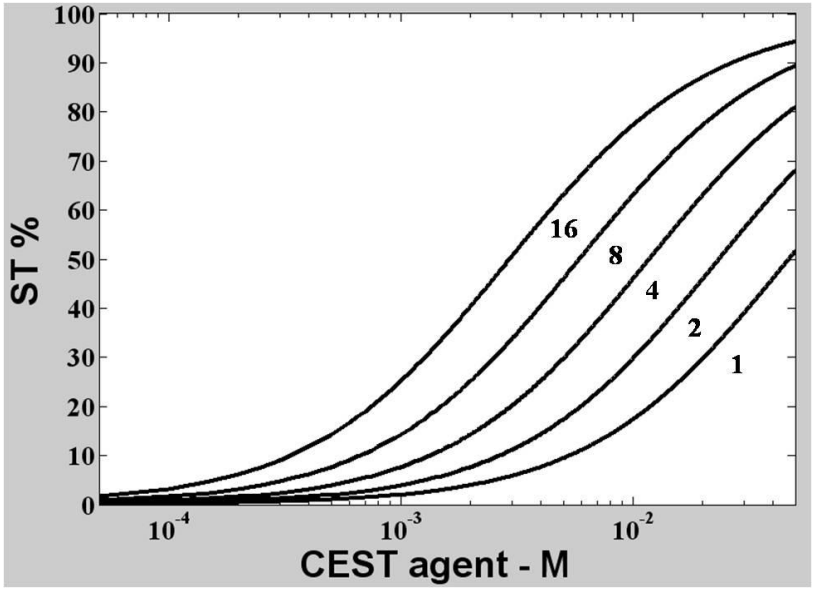

The number of mobile protons for Large Unilamellar Vescicles (LUV) range from $2{,}4 \times 10^6$ (50 nm) to $2{,}1 \times 10^9$ (500 nm)

⇓

Liposomes can be very efficient CEST Probes

k_{ex} can be modulated by:

- varying the liposome membrane permeability (P)

(k_{ex}= P × S/V)

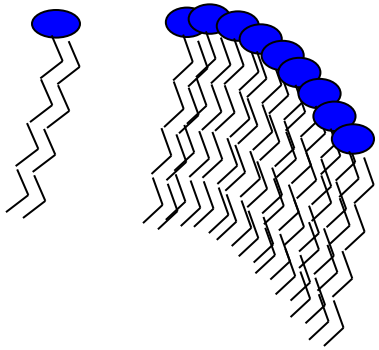

Saturated phospholipids
Membrane tightly packed
Slow exchange

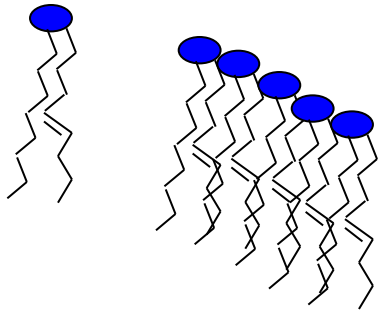

Unsaturated phospholipids
Less tightly packed
Fast exchange

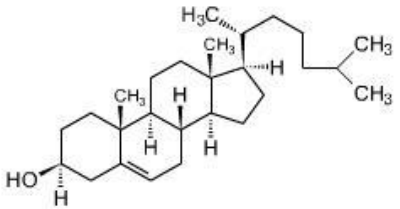

Cholesterol insert himself
in the hole
Reduce the exchange rate

- Varying the liposome size (k_{ex}= P × S/V=P x 3/radius)

k_{ex}

n° of mobile protons

How the resonance frequencies of inner and outer water protons can be separated ?

Encapsulating a paramagnetic shift reagent (SR) in the liposome

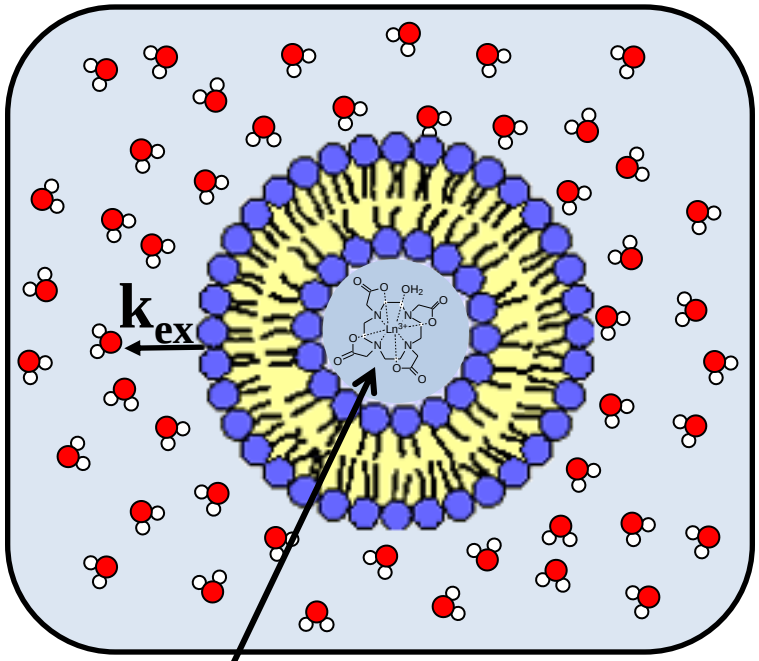

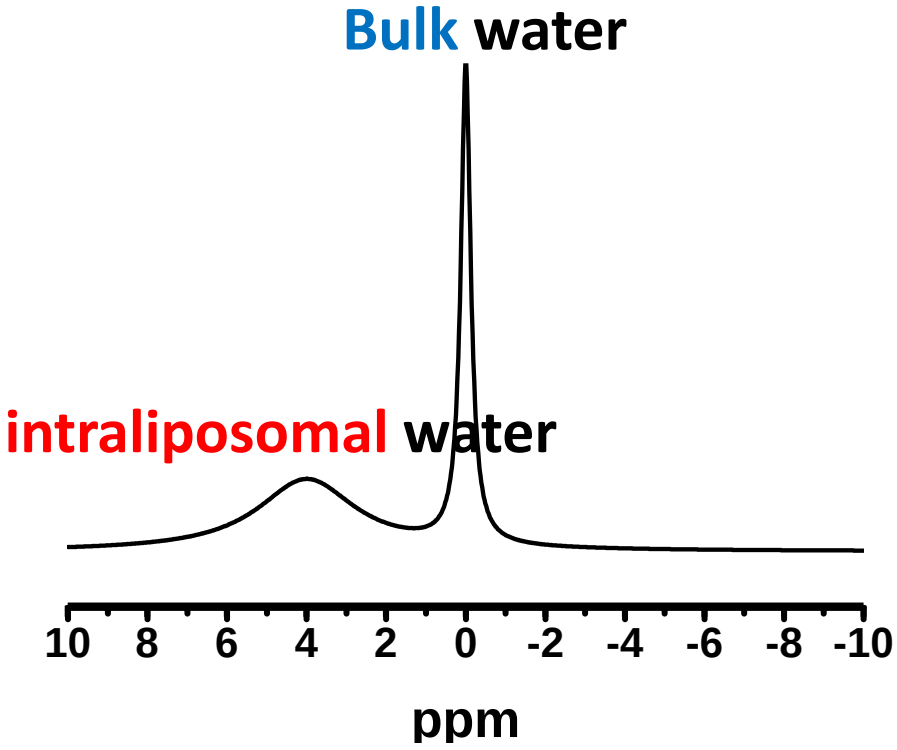

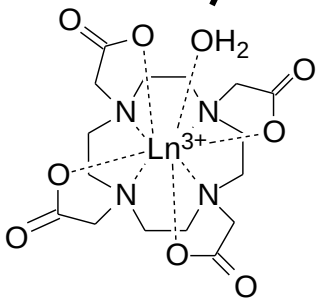

Lanthanide-based SR

Angew. Chem. Int. Ed., 2005, 44, 5513.

The chemical shift of the water protons (δ) in the presence of a paramagnetic SR is the sum of three contributions:

$$\delta = \delta_{DIA} + \delta_{HYP} + \delta_{BMS}$$

δ_{DIA} often negligible

δ_{HYP} requires a "chemical" interaction between the paramagnetic center (the Ln(III) ion) and the water molecule

(through bond: contact shift; through space: pseudocontact shift)

δ_{BMS} does not require a "chemical" interaction and it is dependent on the bulk magnetic susceptibility of the compartment containing the SR

In the case of spherical compartment δ_{BMS}=0 →

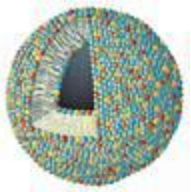

Conventional liposomes

Shift Reagent for intraliposomal water protons

When $k_{ex} >> \Delta\omega$ then:

$$\delta_{\substack{intralipo \\ water}} = \frac{[H_2O]_{bound\ to\ SR}}{[H_2O]_{total}} \times \delta_{\substack{bound \\ water}}$$

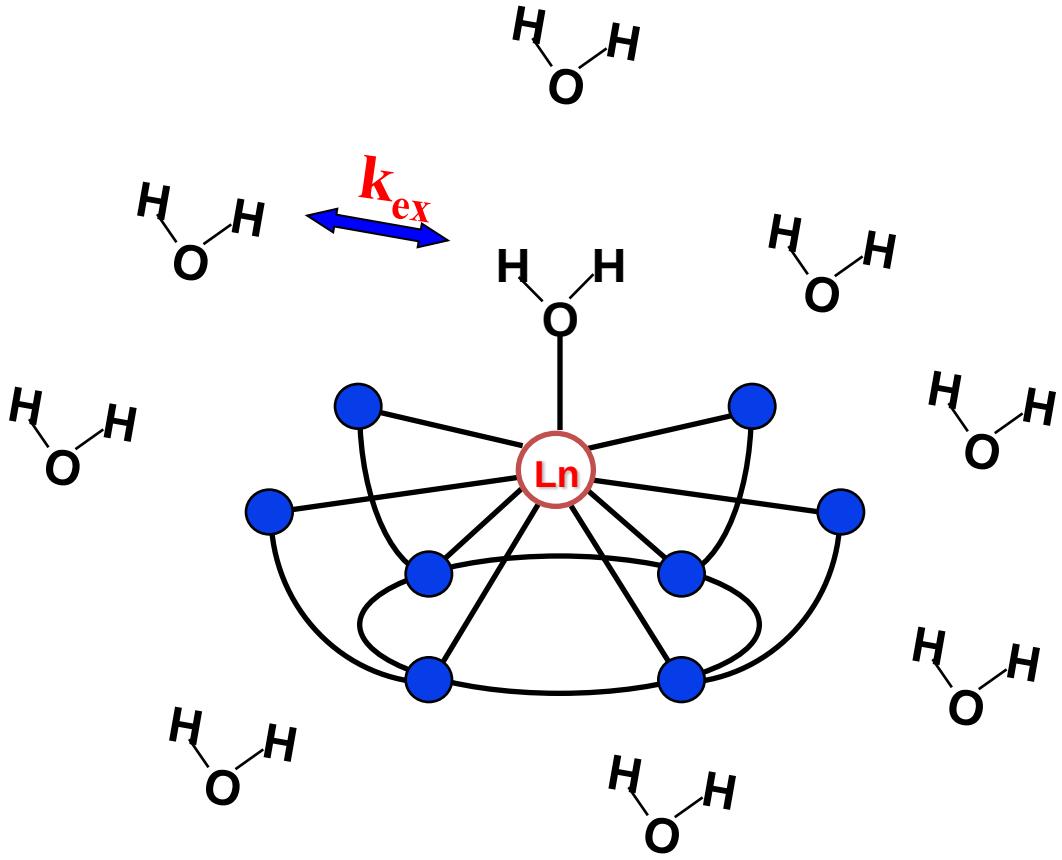

$$\delta_{\substack{bound\\water}} = \delta_{HYP} = \delta_{\substack{pseudo\\contact}} \propto \Delta\chi \times G$$

- $\Delta\chi$ is the magnetic anisotropy of the lanthanide complex Ln

$$\Delta\chi = C_J \times A_0^2 \langle r^2 \rangle$$

- C_J is a constant of the metal

$C_J > 0$ for Eu, Er, Tm e Yb

$C_J < 0$ for Ce, Pr, Nd, Sm, Tb, Dy and Ho

$C_J = 0$ for Gd

- $(A_0^2 \langle r^2 \rangle)$ depends on the crystal field

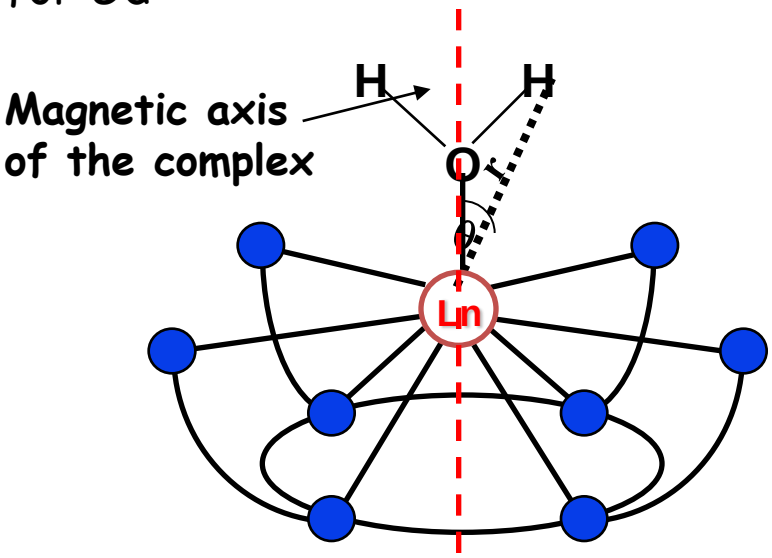

- $G \propto \frac{3\cos^2\theta - 1}{r^3}$

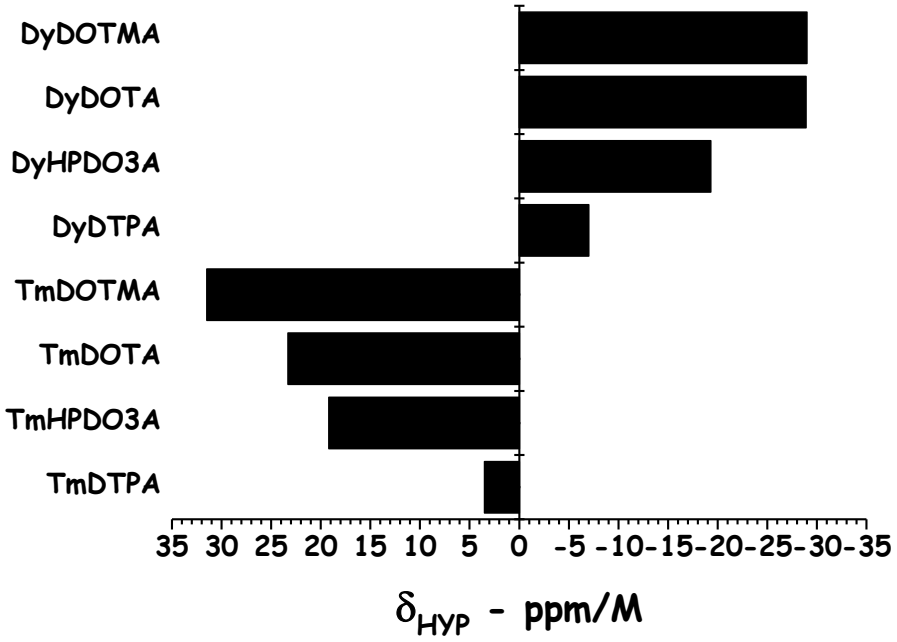

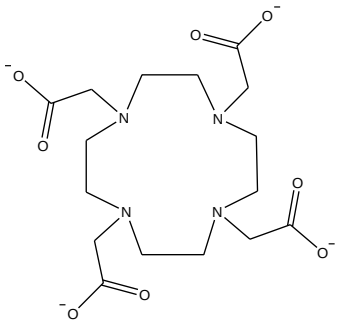

DOTA

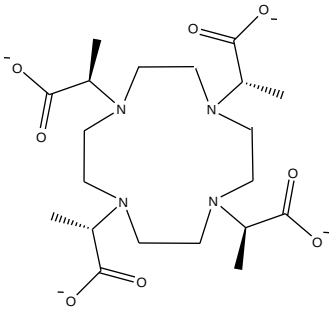

DOTMA

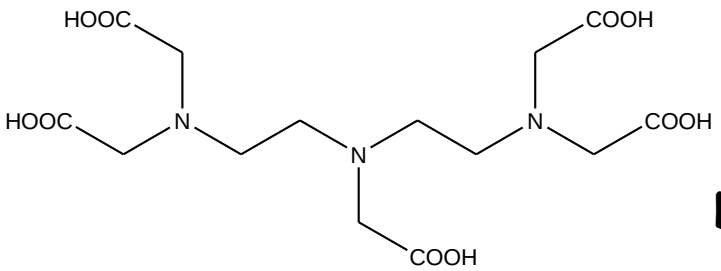

DTPA

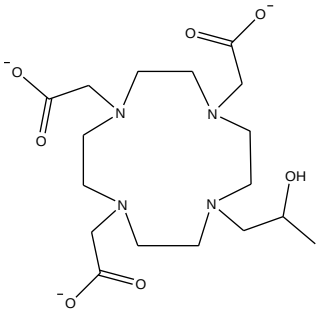

HPDO3A

-Shift differences are due to the geometric differences among the complexes (parameter G)

LIPOCEST agents

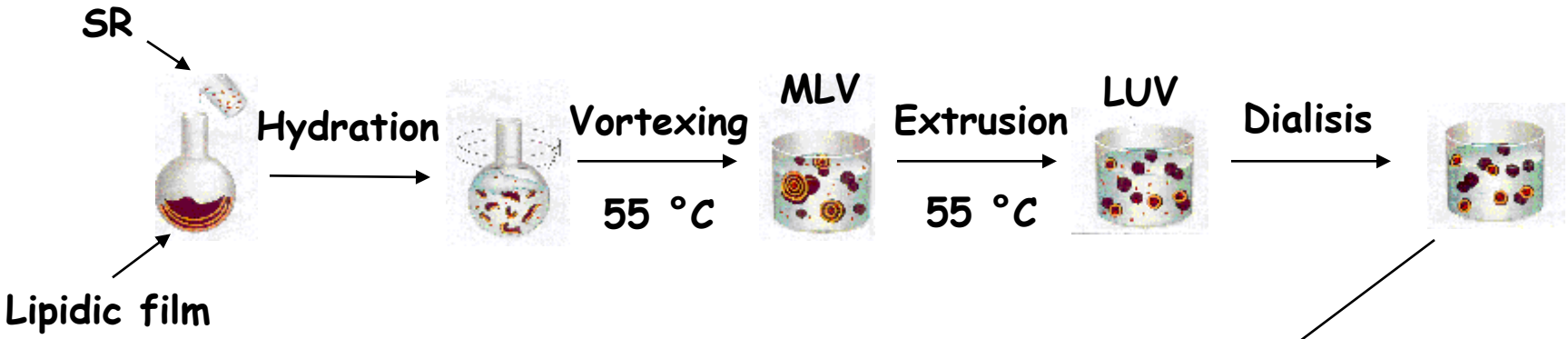

SR unit

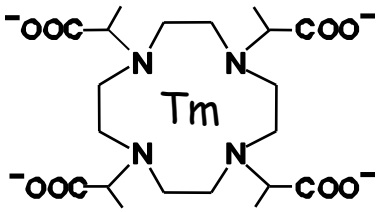

[TmDOTMA]$^-$

0.12 M inside liposomes

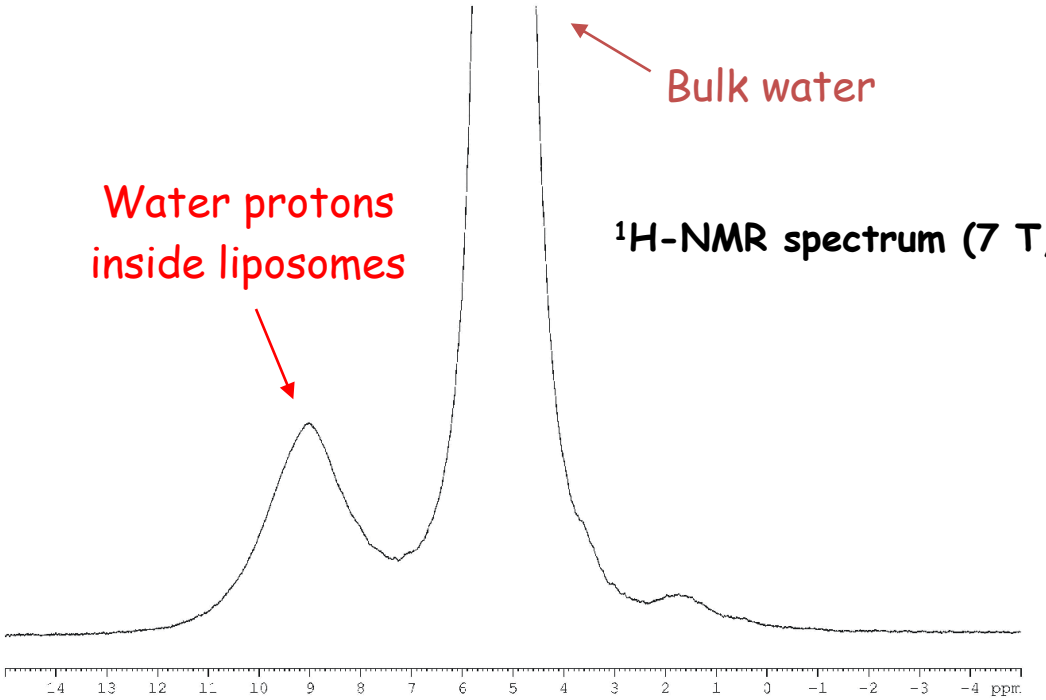

^{1}H-NMR spectrum (7 T, 298 K)

DPPC/DPPG 95/5 (w/w) liposomes

LipoCEST agents: sensitivity

LipoCEST formulation: POPC/DPPG/Chol (55/5/40 in moles) size:250 nm

Experimental condition: 7 T – 37°C – pH 7.4 - B_2 field 6 μT

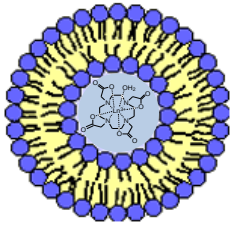

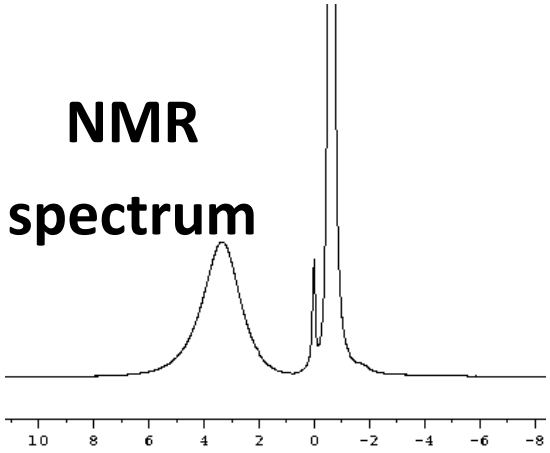

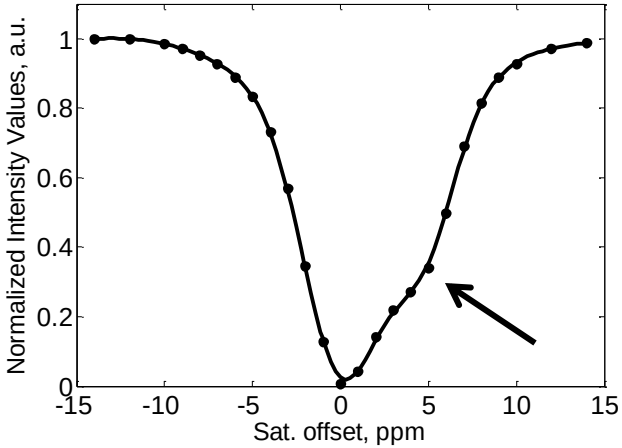

Z-spectrum sample 1

LipoCEST conc.

1. **1.5 nM**
2. **750 pM**
3. **320 pM**
4. **160 pM**
5. **80 pM**
6. **40 pM**

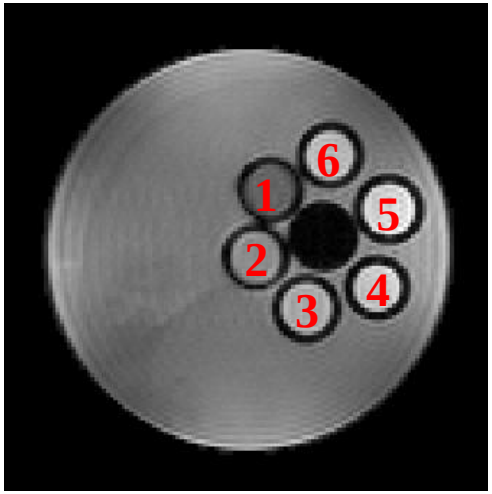

T_{2W} Image

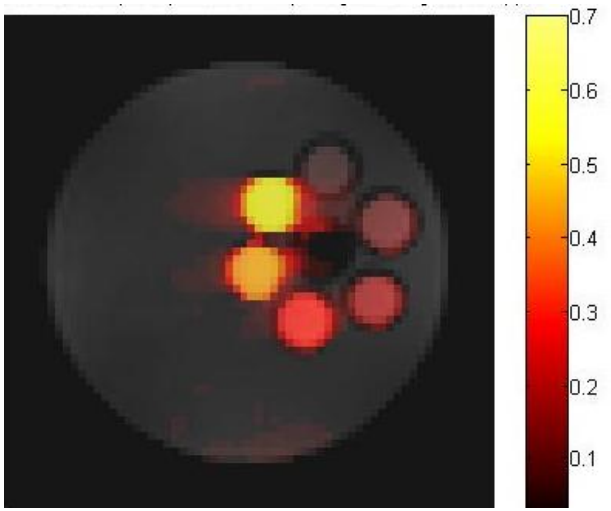

CEST map @ 3.8 ppm

LipoCEST agents: factors affecting sensitivity

- Water permeability of the liposome bilayer (P_w)

Can be modulated by changing the packaging properties of the phospholipids

Phospholipids with saturated aliphatic chains (e.g. di-palmitoyl) displays lower P_w than unsaturated ones (e.g. di-oleyl)

Cholesterol intercalates in the bilayer and reduces P_w

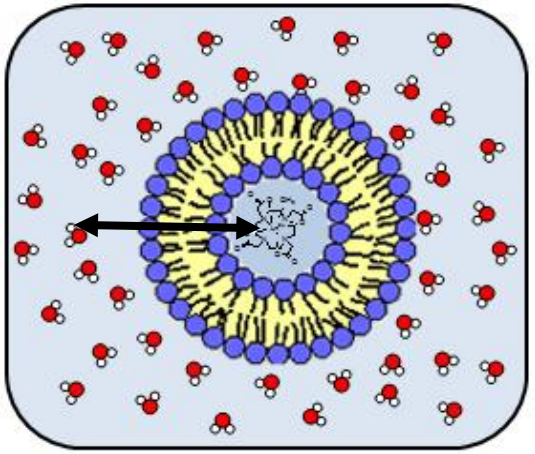

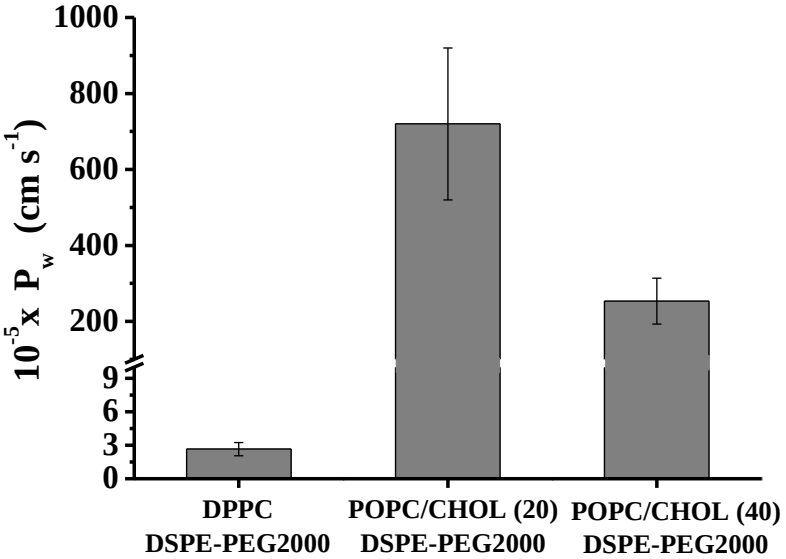

J. Inorg. Biochem., 2008, 102, 1112.

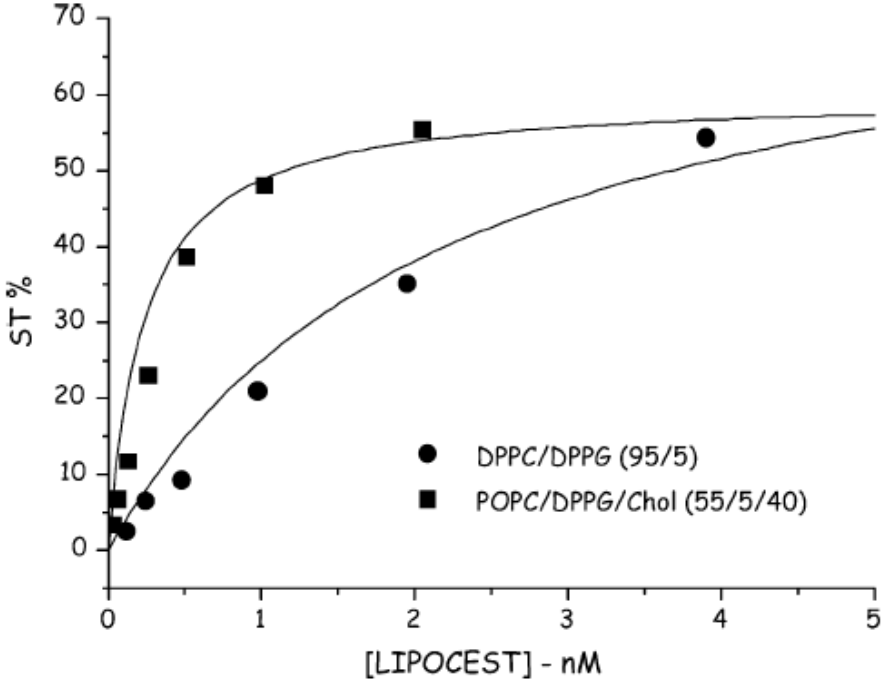

First generation LIPOCEST: spherical liposomes

Pro: Highly sensitive (pM range)

Con: Little frequency range

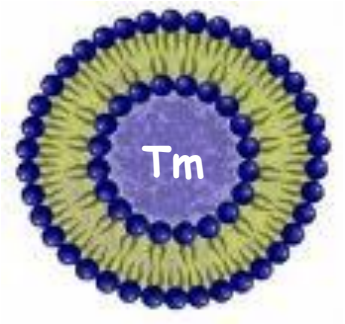

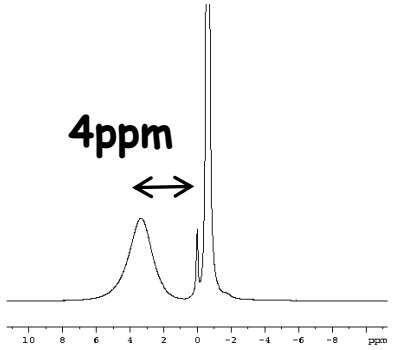

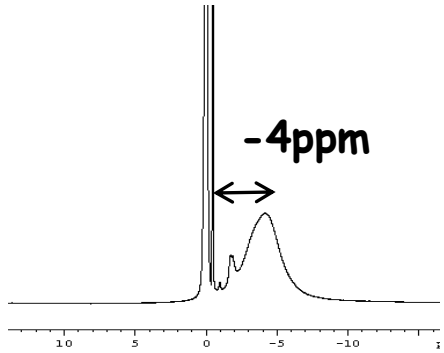

How to increase the shift? → Exploiting the BMS shift

$$LIS_{\substack{Bulk \\ water}} = BMS + Dip$$

BMS depends on the concentration of the shift reagent and its sign depends on the shape and orientation (wrt B_0) of the compartment in which the shift reagent is confined

Second generation of LIPOCEST: non-spherical liposomes

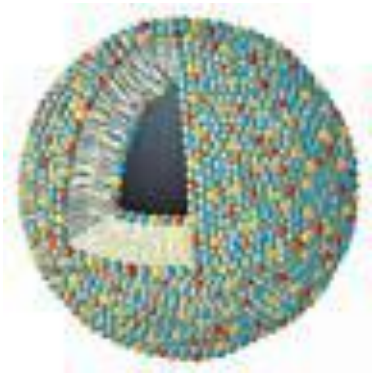

Osmotic shrinkage

$-H_2O$

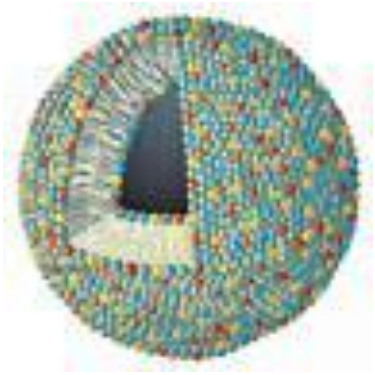

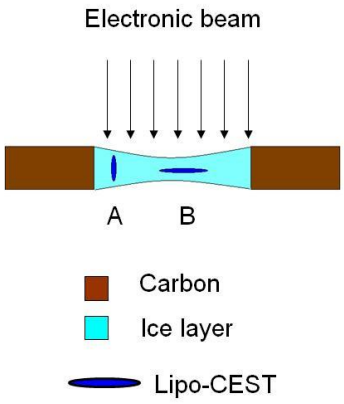

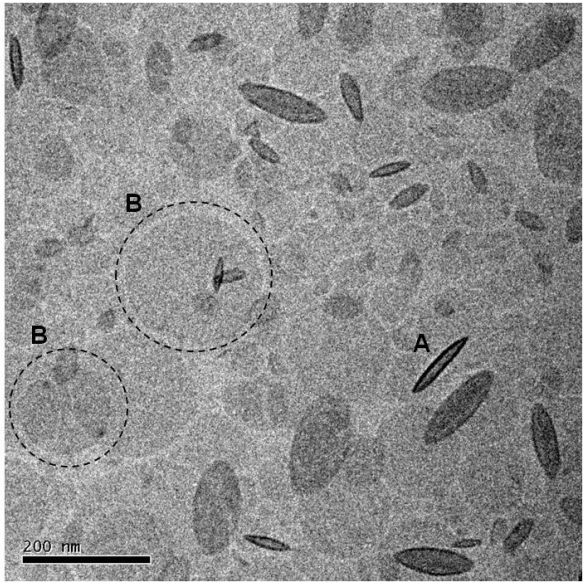

Cryo-TEM images of osmotically shrunken LIPOCEST agents

in collaboration with E. Sanders and N. Sommerdijk from University of Eindhoven (NL)

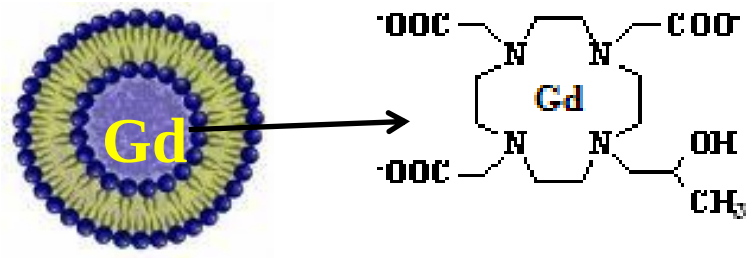

[GdHPDO3A]

Before dialy...

$$C_j\,\mathrm{Gd}=0 \Rightarrow \Delta\chi = 0 \Rightarrow \delta_{\substack{bound\\water}} = \delta_{dia}$$

Gd(III)-complexes has Dip = 0

$$BMS \propto [SR] \times \left(\mu_{eff}\right)^2$$

μ_{eff} Gd = 7.94

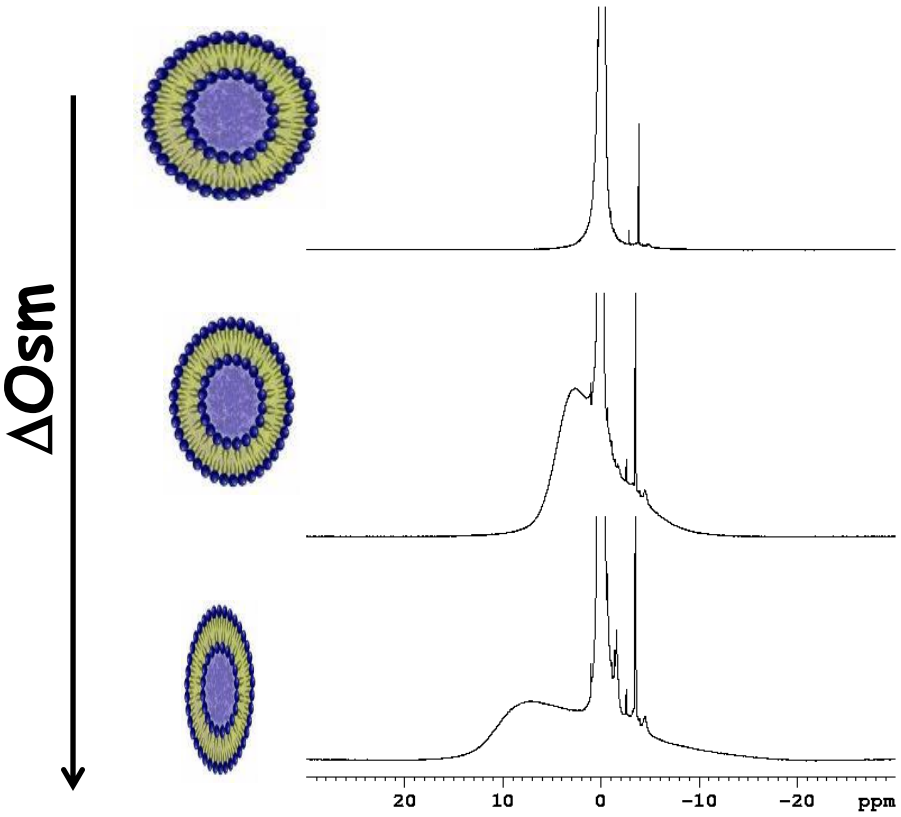

Lanthanides showing the **higher** values for μ_{eff}:

Gd, Tb, Dy, Ho, Er and Tm

Aime S. et al., J. Am. Chem. Soc., 2007, 129, 2430

Hydrophilic SR

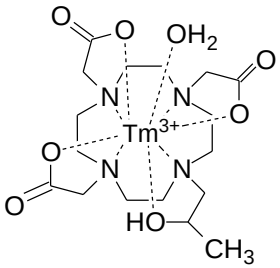

2nd generation

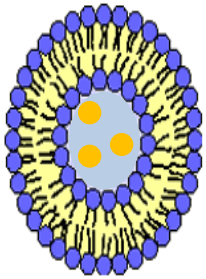

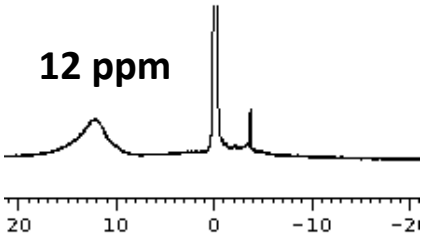

$$LIS_{\substack{int\,ralipo \\ water}} = Dip + BMS$$

Amphiphilic SR

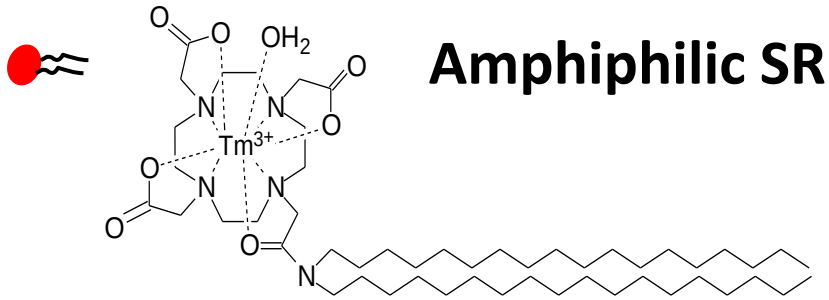

3rd generation

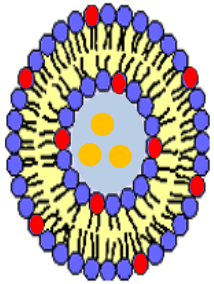

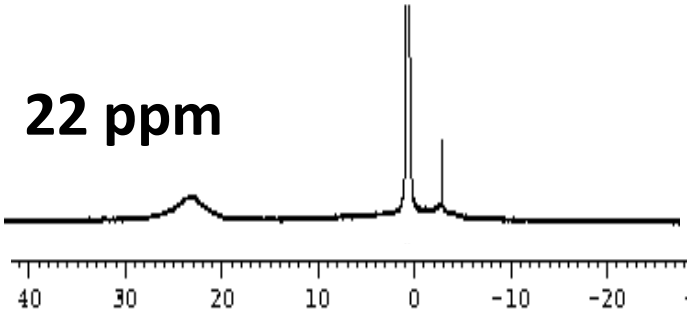

Terreno E. *et al., Angew. Chemie Int. Ed., 2007, 46, 966.*

A further Δ^{LIPO} increase can be achieved by encapsulating neutral multimeric SRs

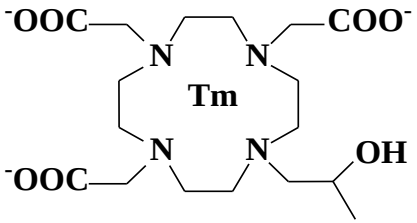

[Tm-HPDO3A]

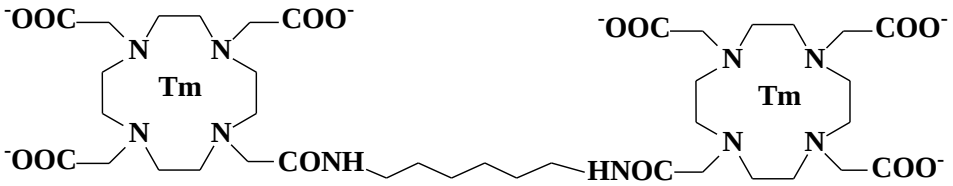

[Tm-dimer]

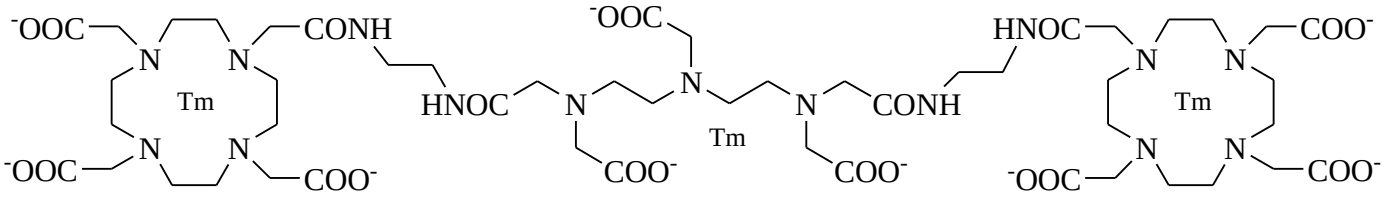

[Tm-trimer]

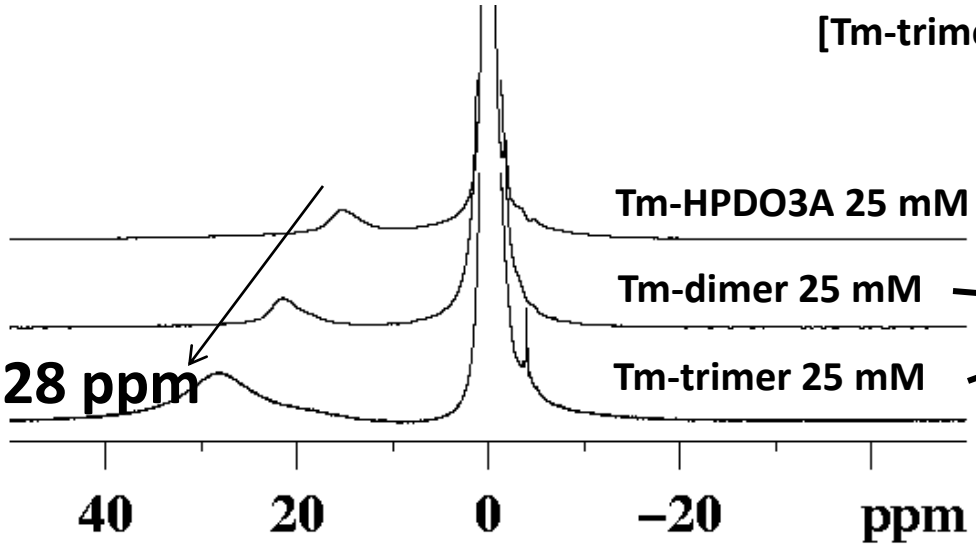

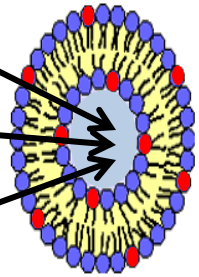

DPPC/Tm-1/DSPE-PEG2000
(75/20/5 mol %)

Terreno E. *et al., Chem. Commun.,* 2008, 600

In addition to increase the magnitude of $\Delta^{LIPO,}$ the incorporation of amphiphilic SRs may also affect he sign of the shift through the modulation of the magnetic alignment of the vesicles.

The sign of the BMS contribution depends on the orientation of the compartment with respect to the external B_0 field

For a cylinder

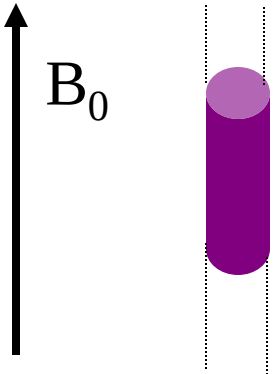

$\Delta^{BMS} > 0$

$\Delta^{BMS} < 0$

As non-spherical vesicles, also the osmotically shrunken LIPOCEST could orient themselves in the field, thus changing the Δ^{LIPO} sign

Phospholipid-based systems, e.g bicelles, are oriented in the field with their principal symmetry axis perpendicular to B_0

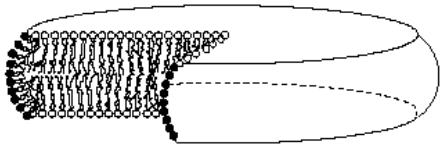

bicelle

The driving force of the orientation is the interaction between B_0 and the magnetic susceptibility anisotropy ($\Delta\chi$) of the phospholipidic membrane.

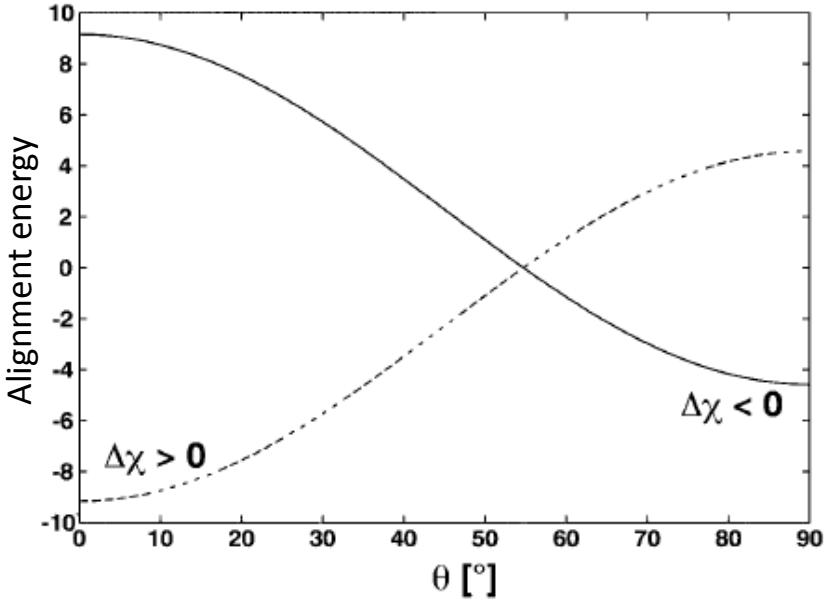

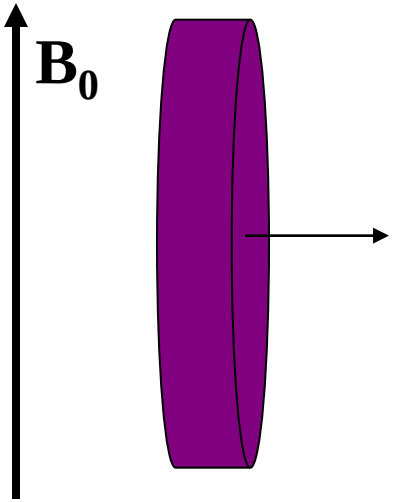

$\Delta\chi < 0$

Incorporation in the membrane of a lanthanide complex with

$\Delta\chi > 0$

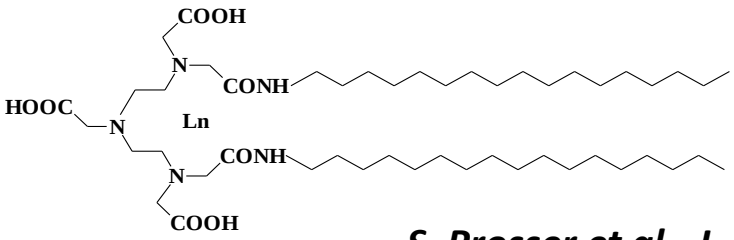

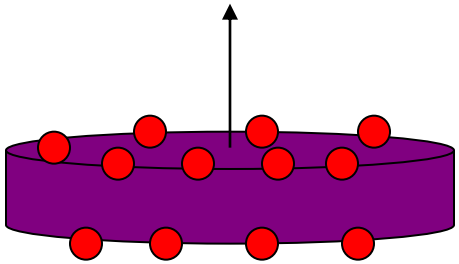

$\Delta\chi > 0$

S. Prosser et al., J. Magn. Res., 1999, 141, 256.

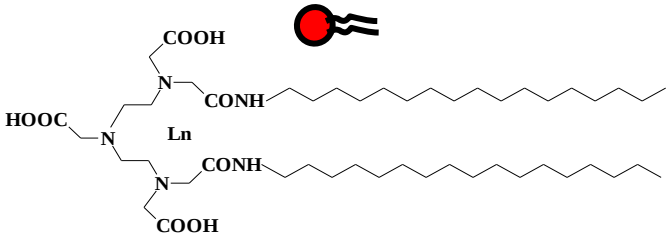

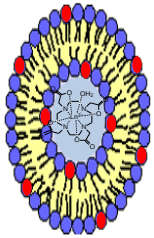

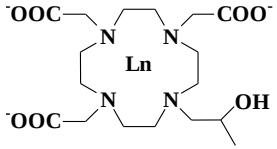

[LnHPDO3A]

$$(\Delta\chi)^{SR} = C_j^{Ln} \times A_0^2 \langle r^2 \rangle$$

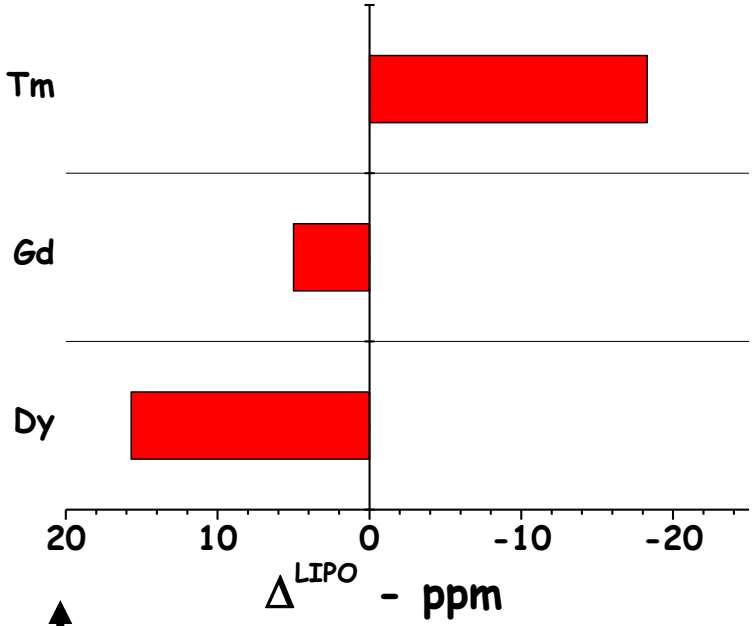

Tm $C_J > 0$ $(\Delta\chi)^{SR} > 0$ $(\Delta\chi)^{LIPO} > 0$

Gd $C_J = 0$ $(\Delta\chi)^{SR} = 0$ $(\Delta\chi)^{LIPO} < 0$

Dy $C_J < 0$ $(\Delta\chi)^{SR} < 0$ $(\Delta\chi)^{LIPO} < 0$

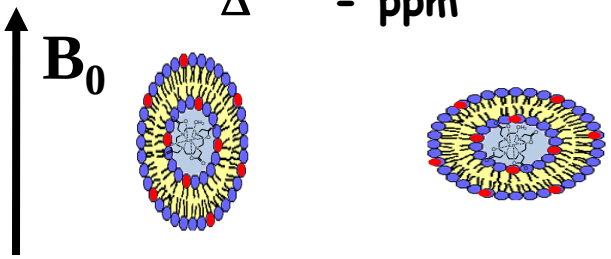

$(\Delta\chi)^{LIPO} < 0$ $(\Delta\chi)^{LIPO} > 0$

with the same amphiphilic ligand it is possible to change the liposome orientation by changing the Ln(III) ion

[Tm-HPDO3A]

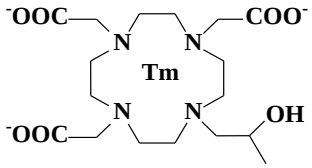

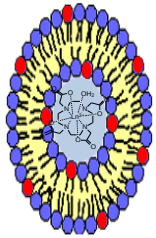

$$(\Delta\chi)^{SR} = C_j^{Ln} \times A_0^2 \langle r^2 \rangle$$

Tm $C_J > 0$

Tm(III) complexes

1

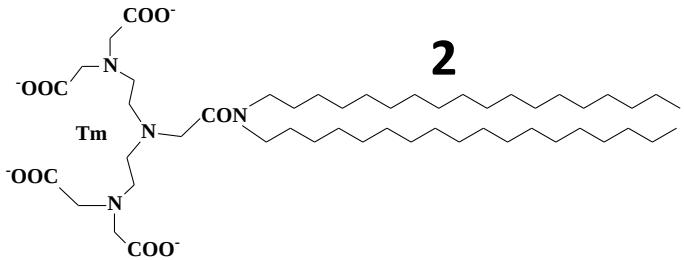

2

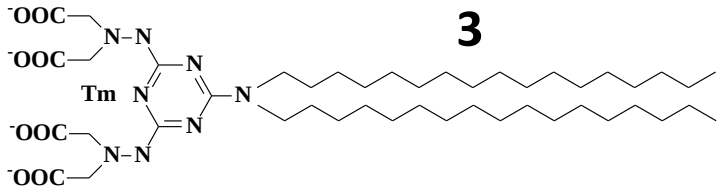

3

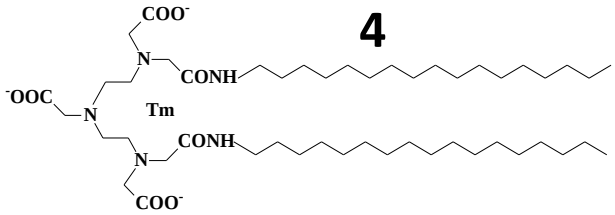

4

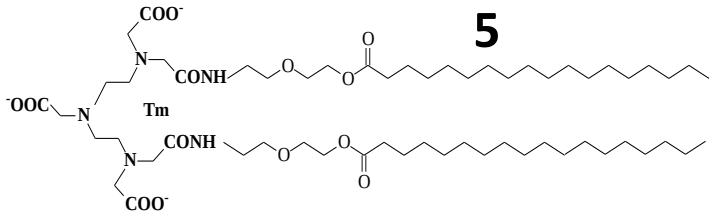

5

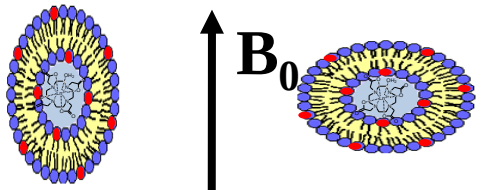

$(\Delta\chi)^{LIPO} < 0$ $(\Delta\chi)^{LIPO} > 0$

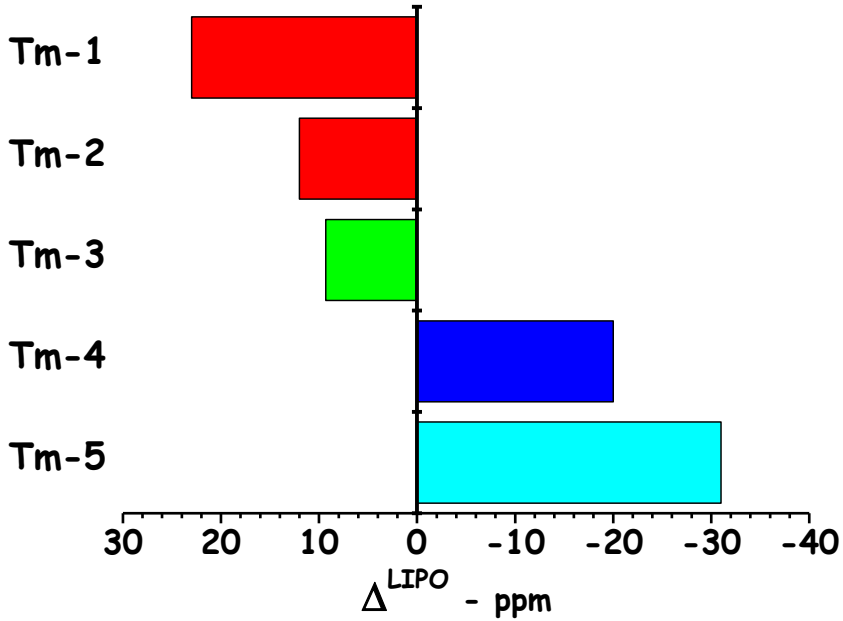

Delli Castelli D. *et al., Inorg. Chem., 2008, 47, 2928.*

Extending the range of Δ^{LIPO} values

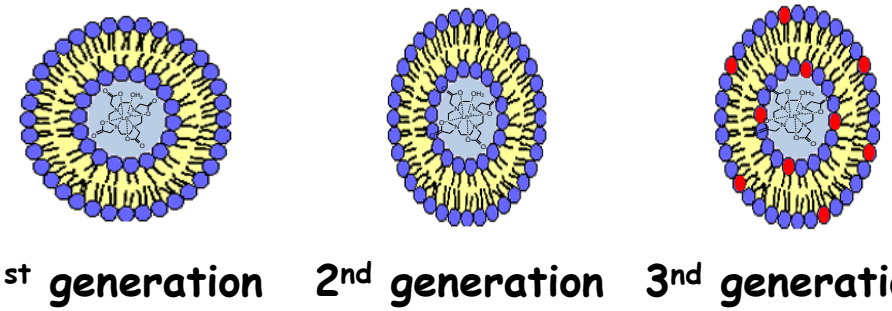

1st generation 2nd generation 3nd generation

Δ^{LIPO}

Entrapping monomeric or multimeric neutral hydrophilic shift reagents

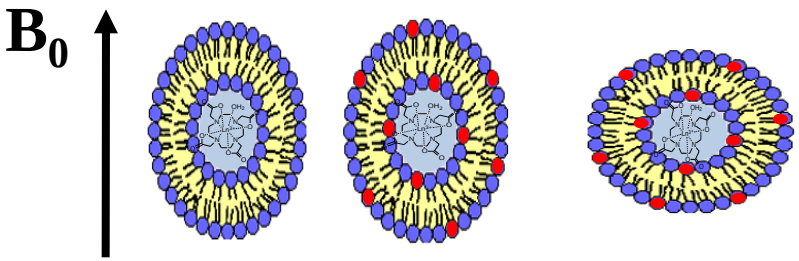

$\Delta^{LIPO} > 0$ $\Delta^{LIPO} < 0$

The Δ^{LIPO} sign for not spherical LipoCEST agents depends on their orientation in the B_0 field

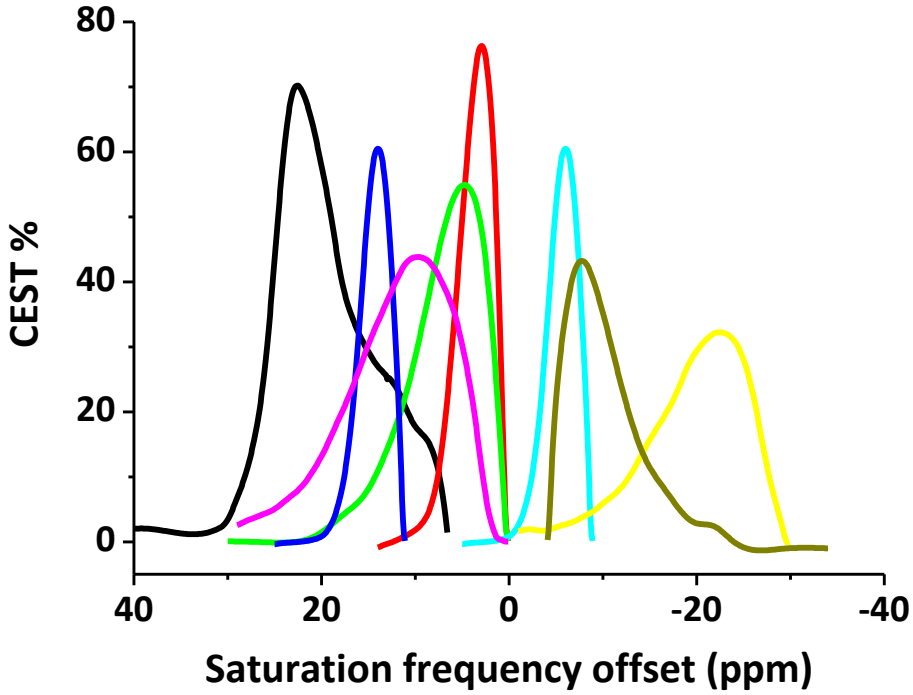

Terreno E. *et al., Methods Enzymol. , 2009, 464, 193.*

Multiple detection of LipoCEST agents: buffer vs. agar

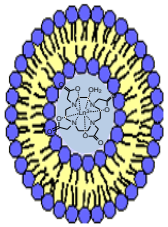

A

Δ^{LIPO} 6.7 ppm

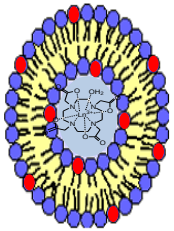

B

Δ^{LIPO} 18 ppm

7 T – 312 K – sat. intensity 6 μT

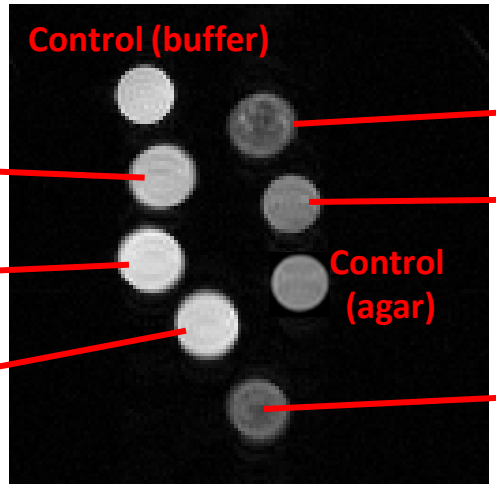

In buffer

A + B

A

B

A

B

A + B

In agarose gel

6.7 ppm

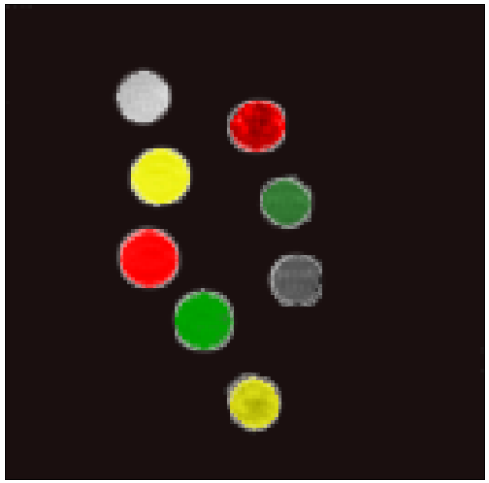

@18 ppm

In vivo Multiple detection of LipoCEST agents

Subcutaneous injection

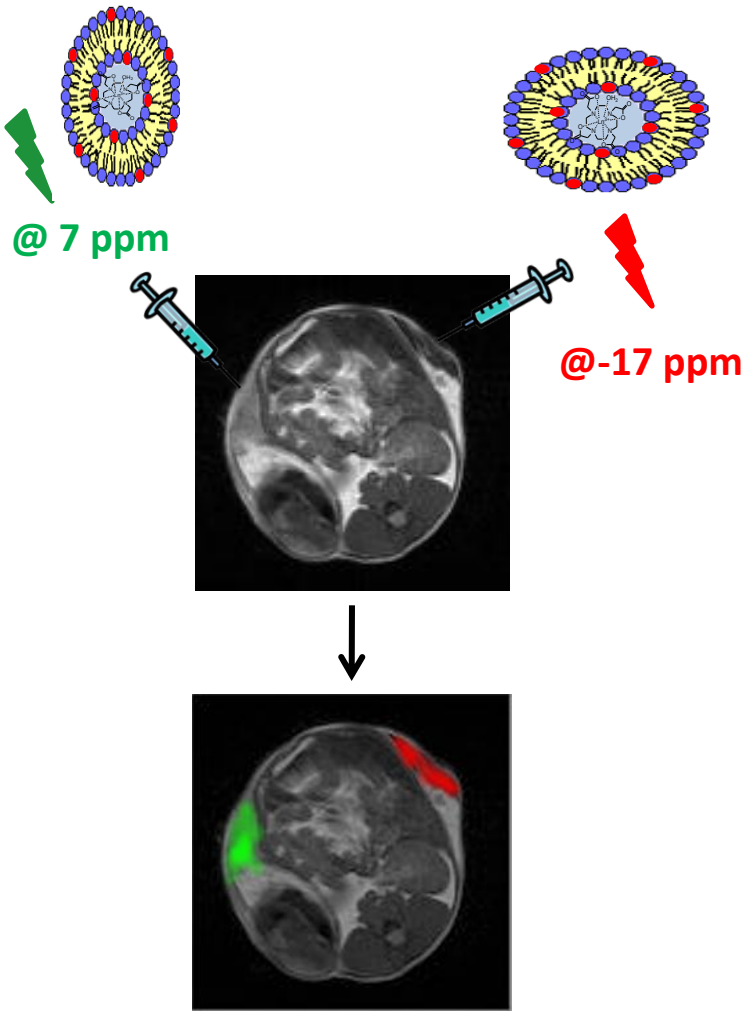

Intramuscolar injection

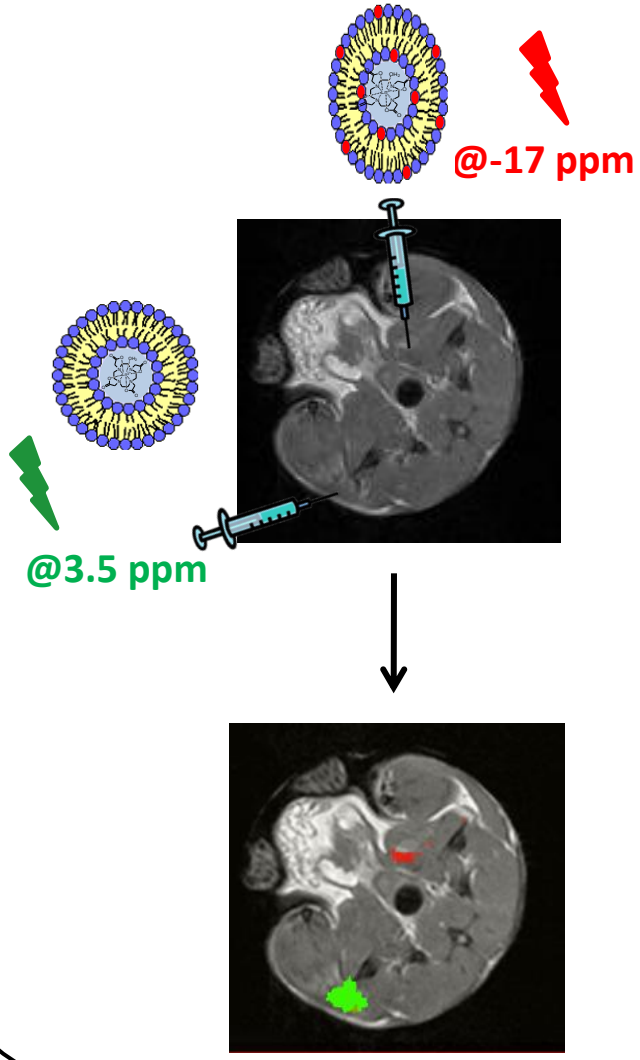

Some readings…

S. Zhang et al., *Acc. Chem. Res., 36, 783, 2003*

- M. Woods et al., *Chem. Soc. Rev., 35, 500, 2006*

- J. Zhou et al., *Progr. NMR Spectr., 48, 109, 2006*

- S. Viswanathan et al., Chem. Rev., 110, 2960, 2010

- E. Terreno et al., *Contrast Media Mol. I., 5, 78, 2010*

- Hancu I. et al., *Acta Radiol., 51, 910, 2010*